Model equations of state

A. V. Bushman and V. E. Fortov

Institute of Chemical Physics, Academy of Sciences of the USSR
Usp. Fiz. Nauk **140**, 177–232 (June 1983)

Model equations of state determining the thermodynamic characteristics of matter in various states of aggregation are reviewed. Methods for describing the thermodynamics of gases, liquids, and plasmas are described. Quantum-mechanical models for solids and a quasiclassical model of matter are discussed. Models which can be used to study melting, evaporation, structural and electronic phase transitions in solids, and phase transitions in nonideal plasmas are also discussed. The ranges of applicability of the various methods are determined. The results of model-based calculations are compared with the experimental data available.

PACS numbers: 64.10. + h, 64.70. – p, 05.70.Ce, 52.25.Kn

CONTENTS

1. INTRODUCTION

Researchers from a wide variety of disciplines have always been concerned with equations of state, which are fundamental characteristics of substances, determining whether the formal general apparatus of thermodynamics and gas-dynamics can be applied to specific physical systems. Interest in equations of state has recently risen sharply, apparently for two basic reasons.

The development of high-power sources of concentrated energy (lasers; electron, ion, and neutron beams; shock and electromagnetic waves; etc.) has made it possible to study states of matter at extremely high pressures and temperatures which were previously inaccessible, so that the corresponding regions of the phase diagram have not previously been mapped. This development has significantly increased the number of researchers working in the physics of high energy densities—a scientific field which, for the most part, has previously attracted the interest only of astrophysicists. In addition, progress in numerical methods for powerful new computers has led to the development of efficient difference schemes for calculations dealing with time-dependent gasdynamic phenomena. The effect has been to increase sharply the requirements imposed on a description of the thermodynamic properties of a substance, since the accuracy of gasdynamic calculations is determined primarily by the errors of the equation of state for the particular medium.

Thermodynamic characteristics of various substances must be calculated in order to solve essentially any problem in the contemporary physics of high energy densities—in the effort to achieve controlled fusion, to design high-power MHD generators, to carry out calculations on the dynamics of strong shock waves, for the protection of space vehicles from meteoroids, and for determining the structures of stars and planets. These problems, along with the problems involved in the promising technology of high pressures (the synthesis of diamond phases of graphite and boron nitride; explosive, electron-beam, and laser welding and machining of metals; etc.), have provided a powerful stimulus for active experimental and theoretical research. The goals of this research have been to move into unexplored regions of the phase diagram and to obtain more-detailed information in the regions of the phase diagram which have already been explored.

The basic difficulty confronting a systematic theoretical calculation of the equation of state of a substance by the methods of statistical physics is the need to incorporate correctly the structurally complicated interparticle interaction in the quantum-mechanical many-body problem at arbitrary values of the coupling constant. The calculations must therefore deal with simplified models whose ranges of applicability are limited and are determined in each particular case, either from the internal characteristics of the model or through a comparison with more accurate solutions or experimental data. The last approach is obviously the most constructive, since there are many well-known examples (the van der Waals theory, nonideal plasmas, etc.) in which the actual range of applicability of the models goes well beyond the boundaries within which the corresponding small parameters of the models are in fact small.

In the next stage of the development of the thermodynamic models, the experimental data available are used to choose the basic numerical parameters in the func-

 0038-5670/83/060465-32$01.80 © 1984 American Institute of Physics

tional dependences constructed from the exact solutions. The semiempirical models obtained in this manner are used to describe and formulate suitable zeroth-order approximation models in particularly complicated situations (liquids, solids, and dense plasmas) where no small parameter can be found for a perturbation theory. The success of the semiempirical models is measured by how well they describe various types of experimental data, over as broad a range as possible, and also by whether they support extrapolation calculations. Clearly, experiments are not merely a necessary supplement to the semiempirical models but in fact the very basis for their existence.

Finally, a large part of the state diagram of a substance—and a part important for practical applications—is presently inaccessible both theoretically and experimentally. The situation provides a fertile soil for the growth of a wide variety of hypotheses, usually formulated in terms of heuristic models which are extrapolations into the highly nonideal region of results of a simpler calculation carried out for slight deviations from the ideal. Models of this sort, which are qualitative and do not come close to being quantitative, frequently predict new phases and states with exotic properties, demonstrating the need for careful experimental study of regions with important interparticle interactions.

Our purposes in this review are to carry out a comparative analysis of the various thermodynamic models and to discuss their ranges of applicability over broad ranges of the parameters. Since the thermodynamic literature is vast, we will single out the basic ideas underlying the theoretical methods, and we will discuss experimental results only very briefly. We direct the reader interested in the calculation details and exhaustive bibliographies to the specialized reviews and monographs in Refs. 1–9, which contain detailed studies of the properties of media in specific regions of the state diagram and which are addressed to physicists working in the corresponding fields. Since the articles and books on model equations of state make up a long list, we will be citing primarily recent work, which serves as an introduction to the history of the given topic.

We will focus primarily on describing the states which are of the most practical interest for the physics of high energy densities. These are states which have already been reached or can be reached under controlled conditions in the foreseeable future. The ultraextreme astrophysical applications will thus not be taken up here. The thermodynamics of such situations is strongly affected by relativistic effects, strong gravitational and magnetic fields, thermal radiation, the conversions of elementary particles, etc. These extremely interesting questions are discussed in Refs. 20 and 21, where an exhaustive classification of extreme states is presented. We will also omit strength effects in solids and the thermodynamics of chemical compounds.

The phase diagram with which we are left after these exclusions is shown schematically in Fig. 1. A neutral

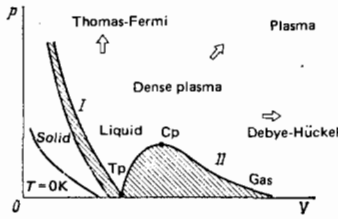

FIG. 1. Phase diagram. Hatched region I—melting; hatched region II—evaporation; Tp—triple point; Cp—critical point; arrows—direction of weakening interparticle interaction.

gas occupies the region of low temperatures and low densities, where the interparticle interaction is weak and can be incorporated in a virial equation of state (Section 2). With increasing density, the strengthening interaction in the system forces us to resort to a purely empirical description, while at supercritical conditions we must deal with models of liquids (Section 6). With increasing temperature, we find a progressive dissociation and ionization of first the outer and then the inner electron shells of atoms (Section 3). The thermodynamic properties of a plasma are described by the equations of ionizational equilibrium, which use experimental data on the spectra of atoms and ions or calculated ionization potentials. The applicability of this approach in the case of low densities is determined by the deviation from the condition of local thermodynamic equilibrium.

As a plasma is compressed, Coulomb-interaction effects strengthen and cause a lowering of ionization potentials. The model of a single-component plasma, a system of point charges in a homogeneous charge-neutralizing background, is widely used to analyze the effects which arise in this situation. Its simplicity makes this model convenient for numerical simulations, and the results can be used to test the various analytic methods used in the thermodynamics of real dense plasmas.

Quantum-mechanical effects are also important in dense plasmas, particularly at low temperatures. A simplified description of quantum effects accompanying the electron-ion interaction based on a binary pseudopotential has made it possible to use the general Monte Carlo method for thermodynamic calculations. It turns out that the characteristics of the pseudopotential for a low-temperature dense plasma can be chosen in a reliable way from experimental data on highly nonideal plasmas.

At higher pressures the strong interparticle interaction affects not only free electrons but also those bound in atoms and ions, thereby deforming the discrete energy spectrum of the plasma. This effect can be described by a model of a bounded atom which effectively incoporates the finite size of the ion and the effect of the plasma environment on the spectrum of this ion.

The structure and thermodynamic description of matter become much simpler at extremely high pressures and densities, where the electron shells of atoms are crushed, and atoms acquire a quasiuniform electron density distribution describable by the quasiclassical

approximation to the method of a self-consistent field (the Thomas-Fermi model; Section 4). A further increase in the density or temperature causes a relative weakening of the Coulomb interaction, so that the equations for an ideal Fermi or Boltzmann electron gas, respectively, can be used. The lower limit on the applicability of the Thomas-Fermi model is determined by the approximate incorporation of the quantum and exchange corrections and the need to take into account the shell structure of the elements.

As the pressure and temperature are lowered, the behavior of the substance becomes determined by the particular shell structure, the way in which the electron energy bands are filled, and the symmetry of the crystal lattice (Section 5). Here it becomes a complicated matter to classify the possible states, and the modern methods of the quantum theory of solids must be used to describe the various situations. At sufficiently high pressures, close-packed structures arise in solids after a series of polymorphic transitions, so that the Wigner-Seitz spherical-cell model can be used. In this model, one seeks a solution of the wave equation using Bloch boundary conditions.

A detailed study of the various aspects of the Fermi surface and a description of loosely packed structures require consideration of the deviations from spherical symmetry and the use of more sophisticated quantum-mechanical models of augmented plane waves and linear muffin-tin orbitals, the Green's-function method, etc. Determining the band structures in these approximations requires laborious calculations, which have been carried out for only a few elements, and in only a limited part of the phase diagram.

The factor primarily determining the thermodynamic properties of the nontransition metals is the particular behavior of the valence electrons, which depends only slightly on the intra-ion potential. It becomes possible to introduce an electron-ion pseudopotential interaction with an extremely simple description of the ion core. The numerical parameters of the pseudopotential are chosen from experimental data on the shape of the Fermi surface. The absence of data of this sort at high pressures and temperatures limits the usefulness of the pseudopotential model over a rather broad range of parameters.

The region of the liquid state (Section 6) has traditionally been considered the most difficult and least studied, since the strong interaction and the disorder render theoretical predications of the properties of real liquids extremely uncertain. It has recently been found possible to formulate some realistic zeroth-order approximation models based on extremely simplified potentials of hard and soft spheres, which allow the use of the numerical methods of molecular dynamics and the Monte Carlo method. Studies by this approach have reproduced the basic qualitative features of the experimentally observed structure factors, and the nature of melting and crystallization has been analyzed (Section 7). The equations of state of real liquids are determined from computer calculations based on a variational method of perturbation theory; the parameters of the binary interparticle potential are found by comparing the calculated results with experimental data. The absence of reliable experimental data at high pressures and temperatures has significantly retarded the development of realistic models for liquids which would work all the way up to the boiling boundary where the liquid converts into a vapor or (in the case of metals) directly into a plasma phase.

The most extensive and reliable experimental results on the equations of state of matter at high pressures, in the condensed phase, have been obtained by dynamic methods based on the use of strong shock waves for the generation of, and the thermodynamic diagnostics of, the resulting states. These experimental results are the basis for semiempirical equations of state (Section 8) which have been constructed from simplified models regarding the thermal-vibration spectrum and the nature of the interparticle interaction in a substance. These semiempirical equations of state contain several adjustable parameters for a quantitative fit of the experimental results. Although these models are definitely empirical, they give a highly accurate description of a large part of the phase diagram, including high-temperature melting and evaporation, and they predict the correct asymptotic behavior in the regions of the Thomas-Fermi gas and the ideal plasma.

It can be seen from this analysis that a rigorous theoretical description of the properties of a substance is possible at extreme pressures and temperatures at the periphery of the phase diagram, while the interior part of the diagram—the most interesting and the most important region in practice—can be described, if at all, only by the model-based theories. This circumstance provides a real stimulus to the active theoretical and experimental research presently being carried out on the physical properties of matter under conditions of strong interparticle interaction.

2. EQUATIONS OF STATE OF GASES

The model of an ideal gas is a first and simplest approximation, applicable at low densities and modest temperatures, where thermal dissociation and ionization do not yet occur in the system and where the energy of the interparticle interaction is small in comparison with the kinetic energy of the particles. The most common method for taking this interaction into account is to use Mayer group expansions, which lead to a virial equation of state[1]

$$P=\frac{NkT}{V}\sum_i\frac{N^iB_i(T)}{V^i}, \tag{2.1}$$

where the virial coefficients $B_i(T)$ incorporate the interaction of the i particles through the potential $\varphi_{ij}(r)$. The shape and the parameters of the potentials φ_{ij} are chosen for a consistent description of information of as many types as possible—data from quantum-mechanical calculations of binding energies, data on the spectra of diatomic molecules, diatomic molecules, data from molecular-beam experiments, and the various types of thermophysical data.

This type of description of a system has been ana-

lyzed for inert gases with exp–6, 12–6, and n–6 potentials, and the parameters and optimum type of potential have been determined.[2] The short-range nature of these potentials means that the integrals in B_i converge, but practical calculations of the higher-order virial coefficients run into difficulties because of the need to evaluate multiple integrals. The first seven virial coefficients have now been calculated for the simple hard-sphere potential, and the first few coefficients have been calculated for a more realistic interaction potential.[2] In the specific calculations, the convergence of expansion (2.1) rapidly worsens with increasing density, forcing us to use a large number of terms in the series, containing unknown higher-order virial coefficients. We wish to emphasize that the convergence of the virial series has been proved only for an extremely low-density gas.

The effects of the nonadditivity of the interparticle interaction become important in dense systems. Within the framework of the three-particle Axelrod-Teller potential,[2]

$$\Delta\varphi_{123} = \nu\,(1 + 3\cos\theta_{12}\cos\theta_{13}\cos\theta_{23})\,(r_{12}r_{13}r_{23})^{-3},$$

these effects change the value of B_3 of argon by 40% at the critical point. These circumstances limit the applicability of the virial equations of state at high gas densities. For this region, many empirical equations, extremely complicated, have been proposed. These equations are a detailed approximation of the experimental data and are convenient for engineering thermodynamic calculations.

In highly compressed gases the energy of the interparticle interaction becomes comparable to the kinetic energy of the particles, and the situation essentially corresponds to the liquid state, although the distinction between a liquid and a gas at supercritical temperatures is of course arbitrary. Physical models based on integral equations and a numerical simulation of highly compressed classical systems are presently being used very successfully to describe such situations. These models will be discussed in Section 6.

3. THERMODYNAMICS OF PLASMAS

As the temperature of a gas is raised, dissociation and then ionization occur, causing free charges to appear in the neutral system. The long-range nature of the Coulomb interaction makes this interaction a governing influence in the thermodynamic properties of a substance over broad ranges of parameters. This long-range nature of the Coulomb potential also causes theoretical difficulties,[4,5] ruling out the application to plasmas of the conventional apparatus of the statistical theory of gases (the corresponding integrals diverge). A regrouping and a summation of the most divergent terms of the perturbation-theory series, however, make it possible to derive final expressions incorporating screening effects. Quantum effects also play a role of fundamental importance in a dense plasma, making it stable and giving it the correct ideal-gas asymptotic behavior at low temperatures.[5]

For the Coulomb potential, the electronic properties of a plasma are characterized by two dimensionless parameters. The first, the "plasma nonideality parameter," is the ratio of the energy of the Coulomb interaction to the kinetic energy ε_K: $\Gamma_D = e^2/r_D\varepsilon_K$ ($r_D = \sqrt{kT/4\pi ne^2}$ is the Debye screening length). The second is the degeneracy parameter ($\lambda_e = \hbar\sqrt{2mkT}$), which determines the importance of quantum-mechanical effects in the system. The relative importance of these effects is shown in Fig. 2, which also shows the ranges of working parameters of the most typical plasma applications.

At high temperatures (regions I and II in Fig. 2), the quantum effects of the interaction of the free charges are inconsequential ($n\lambda_e^3 \ll 1$), and the kinetic energy $\varepsilon_K \sim kT$ is greater than the typical Coulomb energy ($\Gamma_D \ll 1$), so that the model of an ideal Boltzmann plasma can be used. Under this condition, $T \gtrsim$ Ry (region I), ionization is well developed, while at $T <$ Ry (region II) neutral bound states also exist in the system. Calculations of the plasma composition in regions I and II run into no particular difficulties. These calculations are carried out from a chemical model based on the equations for ionizational equilibrium.[4]

With isothermal compression, the Coulomb interaction is intensified in a plasma; in region III the Coulomb energy becomes comparable to the kinetic energy, $\Gamma_D \gtrsim 1$, complicating a correct theoretical description of such states. An important point is that there is a relatively large number of atoms in the system because of the relatively low temperatures, and if these atoms are to be taken into account it is necessary to calculate correctly the discrete spectrum of the compressed plasma. A further compression of the plasma in region III increases the ratio of the Coulomb energy to the kinetic energy, but it simultaneously gives rise to a degeneracy of the electrons, $n\lambda_e^3 \sim 1$. At this point the Boltzmann statistics gives way to Fermi statistics; the scale kinetic energy is $\varepsilon_F \sim \hbar^2 n^{2/3}/2m$; and a further compression of the nonideal plasma (region IV) reduces the relative importance of the interparticle interaction, substantially simplifying the properties of the system in region V. Because of the large mass of the ions, their degeneracy occurs at higher densities, so that the Coulomb interaction remains strong in region V, where we find crystals and liquids, which are described by appealing to the symmetry and the short-range order (Sections 5 and 6).

The best-studied although most simplified model of

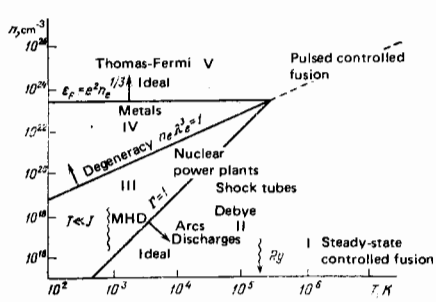

FIG. 2. Typical plasma states.

Coulomb systems is the model of a single-component plasma, which is stabilized by placing it in a homogeneous background of the opposite charge for charge neutralization. There is no recombination in such a plasma, and the nature of the interaction potential raises no doubt.

This plasma model has been the subject of extensive asymptotic theories[22-24] based on expansions in small parameters, regrouping and selective summations of perturbation-theory series, and approximations which borrow the integral-equation technique from the theory of liquids.[25] The standard here is the Monte Carlo method,[26-28] which uses direct computer calculations of the configurational integral, which furnish exhaustive information on the classical single-component plasma over an extremely broad range of the parameter Γ, 0.05–300 [$\Gamma = e^2/kTr_{ws}$, where the average interparticle distance $r_{ws} = (3/4\pi n)^{1/3}$; i.e., $\Gamma = (\Gamma_D^2/3)^{1/3}$], and which are used to construct simple approximate expressions.[28] The screening of the background charges was taken into account in Monte Carlo calculations in Ref. 29 through calculations of the dielectric permittivity of the background in the approximation of a linear response. The analytic methods developed on the basis of a variational principle[30] use a perturbation theory to describe the ion background; calculations from the hard-sphere model are used as a zeroth-order approximation. The results found by this approach are fairly close to those found by the Monte Carlo method, especially at large values of Γ (Fig. 3). It should be noted that the actual calculations of the properties of a single-component plasma frequently use, as a model more realistic than the hard-sphere model, the zeroth-order approximation of the determination of the thermodynamic characteristics of liquid metals (Section 6).

The success of the various asymptotic approximations in extrapolations can be improved dramatically[31] (Fig. 4) by imposing the further requirement that the calculated correlation function obey the condition of local electrical neutrality, corresponding to the equality of the charge of the polarization plasma cloud and the charge of the particle creating this cloud in the plasma. This condition and the analogous conditions imposed on the screening of the dipole and quadrupole moments[31] do not depend on the strength of the interaction in the system; they follow from the fundamental fact that there exists a thermodynamic limit of Coulomb systems.[32] The incorporation of these conditions effectively corrects the approximate correlation functions found from model-based considerations or constructed through expansions in small parameters. We might

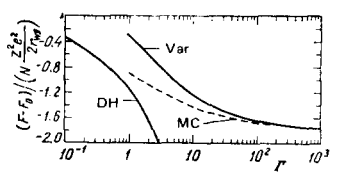

FIG. 3. Free energy of a single-component plasma.[30] MC—Monte Carlo calculations; Var—Variational method (upper boundary); DH—Debye-Hückel law (lower boundary).

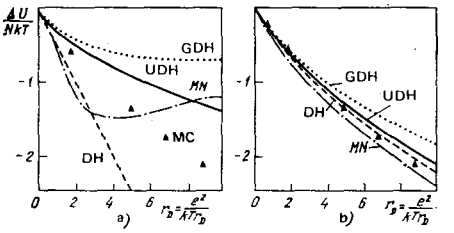

FIG. 4. Interaction energy of a single-component plasma without (a) and with (b) the condition of local electrical neutrality.[31] MC—Monte Carlo calculations; DH—Debye-Hückel law; UDH—unlinearized Debye-Hückel law; GHD—Debye-Hückel law in a grand canonical ensemble; MN—with allowance for the Γ_D dependence of the screening radius.

note that the solution for a single-component plasma of the equations of "superinterlocked" circuits,[25] in which the necessary conditions of a positive correlation function and local electrical neutrality are satisfied automatically, yields results similar to those found from Monte Carlo calculations.

The numerical calculations of the properties of a single-component classical plasma in Refs. 26–28 demonstrate the appearance at a significant compression of thermodynamic anomalies and of a short-range order. These events have been interpreted as a crystallization.[33] According to the recent results of Ref. 28, which incorporate the dependence of the energies of the liquid and solid phases on the number of test particles used in the Monte Carlo method, this transition corresponds in the limit $N \to \infty$ to a value $\Gamma = 178 \pm 1$.

In a real plasma, degeneracy sets in with increasing density, and the interaction is usually described in this case by means of the dimensionless parameter $r_s = r_{WS}/a_0$ (where $a_0 = \hbar/me^2$ is the Bohr radius), which is a measure of the ratio of the average interparticle distance to the atomic distance. This parameter is small in a highly compressed plasma, so that perturbation theory can be used, and the first few terms in the expansion in the coupling constant can be evaluated.[22,34] Wigner[35] has developed a crystal model for a low-density degenerate ($r_s \gg 1$) plasma by assuming that the electron component converts into a face-centered cubic lattice as a result of the strong Coulomb interaction. The properties of this crystal and the conditions for its melting have been studied in detail[36] with allowance for the zero-point and thermal vibrations, anharmonicity, and exchange effects.

The characteristics of a quantum electron plasma have also been found by Monde Carlo methods.[37] These calculations describe a transition from an unpolarized liquid to a ferromagnetic liquid at $r_s > 26$ and a Wigner crystallization at[1)] $r_s > 67$. Dolgov and Maksimov[38] have argued that that estimate is too high; they studied local-field effects and, working in terms of the dielectric permittivity, analyzed the stability of a degenerate electron liquid with respect to the propagation of space-charge and spin-density waves. The particular features of phase transitions in Coulomb systems were analyzed in detail in the review by Iosilevskiĭ,[39] who pointed out that the very conditions for the existence of

a Wigner crystal correspond to a region of thermodynamic instability with respect to the gas-liquid transition. We might note in this connection that as yet there has been no experimental observation of Wigner crystallization in Coulomb systems, and the reports of an experimental observation of a Wigner crystal in experiments using condensed explosives[40] have been shown by further study[41] to have been erroneous.

On the whole, the model of a single-component plasma is effective for calculating the properties of the electron gas in a simple metal, where the energy of the system is determined primarily by the direct Coulomb repulsion between ions and their indirect attraction through conduction electrons[42] (Section 6). Under certain conditions this model also describes the thermodynamics of the plasmas of metal-ammonium solutions, heavily doped semiconductors, the hydrogen-helium plasmas of Jupiter and Saturn, and the nuclear liquid in dense and superdense stars.

The primary shortcoming of the single-component plasma model is its extremely simplified treatment of the charge of the opposite sign, which is taken to be a structureless neutralizing background. Better plasma models attempt to take into account explicitly the structure and the interactions of the charges of all signs. Here it is necessary to describe the quantum-mechanical effects accompanying the Coulomb interaction, which causes a convergence of the coordinate part of the Gibbs probability as unlike charges approach each other and ultimately makes the system stable. Many attempts[4] have been made to retain the classical formalism by cutting off the Coulomb potential at short range and requiring that there be no configurations with charges moving close together. In this approach, the final result incorporates the cutoff parameter. Furthermore, many of these models lose their thermodynamic stability at $\Gamma_D \gtrsim 1$, where the cutoff radius becomes comparable to the interparticle distance.

The systematic quantum-mechanical treatment of the problem works from a Hamiltonian containing the complete interaction among all charges. This approach corresponds to the physical model of a multicomponent plasma, where the discrete spectrum makes a finite contribution, which arises simultaneously with the contribution of the continuous spectrum of the free charges.[5] The physical model is the most general and systematic one for a real plasma, but practical calculations using this model are extremely laborious and have not yet been carried out to any extent,[43,44] since the application of this model to the plasmas of many-electron elements would necessarily require a quantum-mechanical calculation of the internal structure of the bound states.

Configurations with particles moving close together are improbable in a low-density plasma, so that the models can be simplified. The most important simplification is to describe separately the states of the discrete and continuous spectra, which determine the internal structure of the atoms and ions and the behavior of the free particles, respectively. This approximation is the basis for the most popular model in plasma physics, the so-called chemical model, since the number of particles of different species $\{N_j\}$ is determined in this case by the conditions for chemical equilibrium,[3]

$$\sum_j \mu_j = 0, \quad \left(\frac{\partial F(V, T, \{N_j\})}{\partial N_k}\right)_{V,T} = 0, \tag{3.1}$$

and all hypotheses regarding the structure of the particles and their interactions are embodied in the expression for the free energy,

$$F(V, T, \{N_j\}) = F_K + F_d + F_c + F_l.$$

The contribution of the discrete spectrum, F_d, in this model is singled out and calculated without reference to the contribution of the continuous spectrum, which is represented by the kinetic part F_K. The various corrections to the interparticle interaction are described by the term F_c. If the radiation is in local thermodynamic equilibrium with matter, then it is also necessary to take into account the contribution of the energy of the photon gas, which becomes important at extremely high temperatures or at extremely low densities, $F_d = -(4\sigma/3c)VT^4$.

The free energy of the j-th component of an ideal gas is[45]

$$F_k = N_j kT\left[\alpha_j - \frac{f_{3/2}(\alpha_j)}{f_{1/2}(\alpha_j)}\right], \quad f_p(\alpha) = \frac{1}{\Gamma(p+1)}\int_0^\infty \frac{t^p\,dt}{e^{t-\alpha}+1}, \tag{3.2}$$

where the reduced chemical potential $\alpha_j = \mu_j/kT$ is a measure of the degree of degeneracy of the plasma and is determined from the relation $f_{1/2}(\alpha_j) = N_j\lambda_j^3/g_jV$. According to (3.2), incorporating the degeneracy of the electrons lowers the degree of ionization of a plasma, increasing the kinetic part of the electron pressure.

In the spirit of the component composition of the plasma adopted in the chemical model, one singles out the various particular types of interparticle interactions in the calculation of F_c: the atom-atom, electron-atom, ion-atom, and the Coulomb interaction of the charges of the continuous spectrum, which is most characteristic of a plasma. The Coulomb corrections in the chemical model are usually calculated from relations derived for a fully ionized plasma by perturbation theory.[4,5] The primary correction is calculated by summing over the so-called ring diagrams[5]; for a degenerate plasma it corresponds to the Gell-Mann–Brueckner model, and in the Boltzmann limit it leads to the Debye-Hückel model,

$$F_{cr} = -kT\sum_j N_j \frac{\Lambda}{3}\{P(\gamma)\}. \tag{3.3}$$

The dimensionless parameter of the expansion in the perturbation-theory series in (3.3), $\Lambda = V/4\pi NR_D^3$, is directly related to the generalized screening radius $R_D = \sqrt{kT/(4\pi e^2\sum_j Z_jN_j\theta_j/V)}$, where the functions $\theta_j = f_{-1/2}(\alpha_j)/f_{1/2}(\alpha_j)$ reflect the degeneracy of the j-th component, while the factor $\{P(\gamma)\}$ describes the effect of the uncertainty principle in a hot plasma ($e^2Z_j^2/kT \ll \lambda_j$) and corresponds to an effective repulsion of the charges at short range.[5] The term in the expansion following (3.3), calculated for a plasma, is called the ladder term and describes the binary interaction of charges through a dynamic screened Coulomb potential.

Several approximate expressions, with complex structures, have been proposed[45] to take into account quantum-mechanical and diffraction effects in the ladder and following terms of perturbation theory.

In addition to the Coulomb interaction, perturbation-theory methods can be used to calculate the corrections of first, second, and third order for the exchange interaction between free particles of identical spin.[5] The expressions derived by perturbation theory are asymptotic expressions, strictly applicable only at small values of the expansion parameter, $\Lambda \ll 1$. According to Ref. 45, for example, an estimate of the range of applicability of the ring model, (3.3), yields $\Lambda \lesssim 0.5$ ($\alpha_e < 2$), while the more modest estimate $\Lambda < 0.1$ is given in Ref. 5.

In a very nonideal plasma, with $\Gamma_D \gtrsim 1$, the perturbation-theory results do not hold, and it becomes necessary to call upon parameter-free Monte Carlo and molecular-dynamics methods or to use extrapolations. Convenient in the latter approach is the ring Debye approximation in a grand canonical ensemble,[46] which exhibits in the case of a slightly nonideal plasma the correct asymptotic approach to the ordinary Debye approximation, (3.3), while in a very nonideal plasma ($\Gamma_D \gg 1$) it does not cause a loss of thermodynamic stability because of the moderate values of the calculated corrections. This tendency toward a lowering of the corrections has been confirmed independently by results calculated by rigorous asymptotic methods and by various model-based approaches. It has also been confirmed by experiments on the shock compression of nonideal plasmas. Consequently, calculations using the ring Debye model[46] are the most suitable for extrapolating into the domain of highly nonideal plasmas.

The numerical Monte Carlo method has definite advantages for describing the thermodynamic properties of very nonideal plasmas. This method does not involve an expansion in terms of a small parameter, and it proves particularly effective in the cases of dense gases and liquids and also in the case of a single-component plasma—systems in which the interparticle potential is known exactly. This method is based on first principles of statistical physics and involves a direct computer calculation of the average thermodynamic quantities[47]

$$\langle F \rangle \quad Q^{-1}(N, V, T) \int_V \dots \int F_N(\mathbf{q}) \exp[-\beta U_N(\mathbf{q})]\, d^N q, \qquad (3.4)$$

where

$$Q(N, V, T) = \int_V \dots \int \exp\{-\beta U_N(\mathbf{q})\}\, d^N \mathbf{q}$$

is the configuration integral, $\beta = 1/kT$, and the interparticle potential is assumed given, a binary potential in most specific cases,

$$U_N(\mathbf{q}) = \sum_{ij} \Phi(r_{ij}, T), \quad r_{ij} = |\mathbf{q}_i - \mathbf{q}_j|. \qquad (3.5)$$

The use of this technique in the case of a multicomponent plasma runs into some specific difficulties, because it is necessary to incorporate quantum-mechanical effects in the quasiclassical formalism of the Monte Carlo method. These quantum effects play a definite role in a real plasma, giving rise to bound states. In the pseudopotential model of a plasma this difficulty is removed by introducing an effective electron-ion binary potential $\Phi_{ei}(r, T)$, which is determined by equating the quantum-mechanical probability density to the classical correlation function[5,47]

$$g_{ei}(r) = \lambda_e^3 \sum_\alpha |\Psi_\alpha(r)|^2 \exp(-\beta E_\alpha) \equiv \exp[-\beta \Phi_{ei}(r, T)], \qquad (3.6)$$

where Ψ_α and E_α are the orthonormal wave functions and energy eigenvalues, and the summation is over all the states of the discrete and continuous spectra.

The pseudopotential determined in this manner at large values of $r \gg \lambda_e$ agrees with the Coulomb potential, while at $r \to 0$ it has a finite value and depends on the particular electronic structure of the element. This structure is determined by a self-consistent solution of the quantum-mechanical many-body problem and cannot be described by the binary approximation (3.6). Ignoring this fact[47] has led to serious qualitative errors in the model, manifested by the appearance of nonphysical complexes because of an overly deep pseudopotential (3.6).

The model has been improved substantially[47] through the partition

$$\begin{aligned} \exp[-\beta \Phi_{ei}(r, T)] &= S_{ei}^b + \exp[-\beta \Phi_{ei}^*(r, T)] \\ &\equiv \lambda_e^3 \sum_{E_\alpha \leqslant -kT} |\Psi_\alpha(r)|^2 (e^{-\beta E_\alpha} - 1 + \beta E_\alpha) \\ &\quad + \lambda_e^3 \sum_{E_\alpha \geqslant -kT} |\Psi_\alpha(r)|^2 \exp(-\beta E_\alpha), \end{aligned} \qquad (3.7)$$

where the bound states are taken into account through the introduction of the term S_{ei}^b, which determines the partition function of the atom in accordance with Ref. 48, while the continuous spectrum is described by an electron-ion interaction pseudopotential Φ_{ei}^*. The pseudopotentials constructed in this manner depend only slightly on the temperature in the non-Coulomb region; in addition, since the Φ_{ei}^* are determined primarily by hydrogen-like states, they depend only slightly on the particular chemical element. A simple approximation[47] which lies at the basis of the zeroth-order approximation pseudopotential model of a plasma has been proposed[47] on the basis of the similar temperature dependences and the approximate equality, in reduced form, of the pseudopotentials of the various chemical elements[2)]:

$$\begin{aligned} \beta \Phi_{ei}^0(x, T) &= \begin{cases} -\varepsilon & r \leqslant \sigma \\ -x^{-1} & r > \sigma, \end{cases} \quad \sigma = e^2 \beta / \varepsilon, \quad x = r/\beta e^2, \\ \beta \Phi_{ee}^0(x) &= \beta \Phi_{ii}^0(x) = x^{-1}, \end{aligned} \qquad (3.8)$$

where the numerical parameter of this model, ε, is chosen on the basis of experimental data (Fig. 5).

On the whole, the range of applicability of the pseudopotential model of a low-temperature plasma is limited by the neglect of many-particle interactions and the absence of information on the discrete energy spectrum in (3.6)–(3.8). The discrete energy spectrum in a dense plasma may be distorted by the strong interaction, and it is generally not known at the outset. In a weakly ionized plasma, the interactions involving neutral particles become important in addition to the Coulomb interaction. The mutual repulsion is taken into account ap-

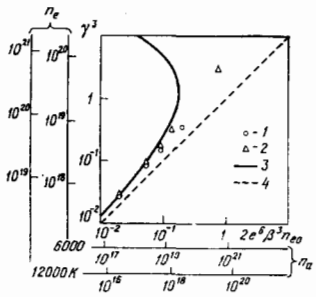

FIG. 5. Equation of ionizational equilibrium in a cesium plasma at $T = 6000$ and 12 000 K (Ref. 47). 1—$\varepsilon = 2$; 2—$\varepsilon = 4$; 3—Debye-Hückel law; 4—ideal plasma.

proximately by means of a model of hard or soft spheres, which incorporates the atomic-volume effects and which leads to a cold pressure-induced ionization at substantial pressures.

In several cases of practical importance, the interaction of charges with neutrals is a governing effect, while the nonideal nature of the charged and neutral components can be ignored. The model of a weakly ionized plasma (an interaction potential $U_{ea} \ll kT$) has been proposed for evaluating the contribution of the electron-atom interaction in this case[49]:

$$\beta\Delta F_{ea} = -4\pi\,|\,a\,|\,\lambda^2 N + 3\frac{\lambda^2}{\lambda_m^2}\left[1 - \frac{4}{3}\pi N\frac{\lambda^2}{\lambda_m^2} f^2(\lambda_m)\right],$$

where

$$\lambda_m = \frac{16\sqrt{\pi\alpha}}{3a_0\,|\,a\,|}\left[1 + \left(1 - \frac{8\alpha}{3a_0\lambda^2\,|\,a\,|^3 N}\right)^{1/2}\right]^{-1},$$

α is the polarizability of the plasma, and $f(\lambda_m)$ is the amplitude for the scattering of an electron with an energy $\hbar^2/2m\lambda_m$ by an atom (experimental data on the transport scattering cross sections can be used to determine this amplitude). The contribution of the ion-atom interaction is described by the polarization model,[49]

$$\beta\Delta F_{ia} = -\beta N\int[e^{-\beta U} - 1]\,d\mathbf{r} \sim -\frac{2\pi\alpha e^2}{R}\beta N,$$

where R is the effective range of the potential $U(\mathbf{r})$. It should be noted that in a highly compressed plasma the interaction of electrons with neutrals can result in localization of the conduction electrons at density fluctuations and can give rise to heavy charged complexes. The cluster model of a plasma has been used successfully to describe the conductivity of metal vapor,[49] but the thermodynamic consequences of the appearance of clusters are less certain.

To take bound states into account appropriately is one of the most complicated problems confronting the development of models for dense plasmas. In the chemical model, the bound states are split off from the continuous spectrum and described by the partition function

$$\beta\Delta F_b = -\sum_j N_j \ln Q_j \qquad \left(Q_j = \sum_{n=1}^{\infty} g_n^j \exp(-\beta E_n^j)\right), \tag{3.9}$$

where g_n^j and E_n^j, the statistical weight and excitation energy, are found either from spectroscopic measurements for a low-density plasma or through quantum-mechanical calculations for the isolated atoms and ions. The partition function of an isolated atom diverges and must be artificially cut off, to reflect the presence of a plasma environment.[4,5] For most substances the energies of the first few excited states are comparable to the ionization potential, so that their contribution to Q_j is important only at high temperatures, where the plasma is significantly ionized and contains few neutrals. Consequently, the specific mechanism limiting Q_j for a low-density plasma is less important than the very fact that the limitation does occur, and this circumstance partially explains why the corresponding models are rather crude approximations. With increasing pressure, the degree of ionization of the plasma falls off, making the thermodynamic functions more sensitive to the specific method used to calculate Q_j and requiring a more careful account of how the nonideal effects influence the bound-state contribution.

In a highly compressed plasma the interparticle interaction causes a significant shift, deformation, and splitting of energy levels—effects which are not described by perturbation theory and which require a complete solution of the quantum-mechanical problem incorporating the interactions of all particles. The models proposed for this situation must determine the characteristics of the discrete spectrum with appropriate allowance for the distortion of the spectrum by the surrounding medium. The simplest approach is to calculate the bound states of one electron in various potentials simulating the plasma surroundings.[50] Graboske *et al.*[51] have studied the thermodynamic consequences of a compression-induced change in the energy spectrum of hydrogen. They showed that at substantial densities the compressibility of a plasma decreases by a factor of more than two because of the deformation of bound states.

A description of the thermodynamic properties of a highly compressed plasma of heavy elements requires calculations of the shell structure of the atoms and ions and incorporation of the effect of the compression on the positions of the energy spectra of the bound electrons. The corresponding calculations can be carried out in the model of a bounded atom,[52] according to which the Z atomic electrons lie inside a spherical cell of radius r_c with an interaction potential

$$U_{ie}(r) = \begin{cases} -Ze^2/r, & r < r_c, \\ \infty, & r \geqslant r_c. \end{cases} \tag{3.10}$$

The radial parts of the wave functions of each electron, φ_{nl}, and the energy levels, E_{nl}, are calculated by the Hartree-Fock method in this model, through a numerical solution of a system of nonlinear integrodifferential self-consistent-field equations (here and in Section 4 we we are using the atomic system of units, with $\hbar = e = k = m = 1$):

$$\left[\frac{d^2}{dr^2} - U_{nl}(r) - \frac{l(l+1)}{r^2} - E_{nl}\right]\varphi_{nl}(r) + \sum_{n \neq n'} \varepsilon_{nl,\,n'l}\varphi_{n'l}(r) = G_{nl}(r); \tag{3.11}$$

here U_{nl} is the Coulomb potential of the interaction of electrons with each other and with the nucleus, (3.10),

G_{nl} is the nonlocal (exchange) part of the potential, and $l(l+1)/r^2$ is the centrifugal potential. The eigenvalues E_{nl} and the off-diagonal Lagrange factors $\varepsilon_{nl,n'l}$ are determined from the orthogonality conditions and the boundary conditions on the wave functions φ_{nl}. The excitation energies E_{nl} found in this manner are used to calculate Q_j in (3.9) and to calculate the free energy, with corrections for the Coulomb interaction and for the interaction of the hard spheres in accordance with Eq. (6.1) of Section 6. The equilibrium radii r_c are determined from the condition $\partial F/\partial r_c = 0$, so that the model is closed from the thermodynamic standpoint.

The results calculated for the energy spectrum of compressed cesium (Fig. 6) clearly illustrate the substantial deformation caused by the compression of first the upper atomic energy levels and then the deeper levels. This deformation reduces the shock compressibility and the internal energy of a dence plasma: an effect which has been clearly seen experimentally.[52,53] According to the calculations of Ref. 52, the distortion of the discrete spectrum of a nonideal plasma is significant under the experimental conditions[3)] (Fig. 6), but it can nevertheless be described qualitatively by such an approximate model as the thermodynamic model of a bounded atom (Fig. 7).

The need to take into account the deformation of the discrete spectrum of a dense plasma is also demonstrated by experiments on the shock compression of metals at ultrahigh pressures. The shock-wave data for thorium at pressures up to 1.5 Mbar and for aluminum and molybdenum up to 10–50 Mbar, for example, can be described successfully[55] (Fig. 8) by a modified ionizational model which incorporates the pressure-induced ionization on compression in addition to thermal ionization. It thus clearly follows that only by taking into account the actual energy structure of the bound states, which stiffen the system, can a model for a dense plasma give a quantitatively correct description of the experimental data. A corresponding conclusion can be reached by examining the results calculated for the thermodynamic properties of a high-temperature condensed phase by band-theory methods (Section 5).

The available experimental methods for studying highly nonideal plasma can detect only overall thermodynamic characteristics. They cannot yield direct information on the relative contributions of the discrete and continuous spectra, especially since these concepts become arbitrary in the case of dense plasmas.[5] At the same time, a model-based interpretation of the experimental data available[52-54] indicates that the Coulomb corrections to the continuous spectrum are smaller than would follow from the ring model, (3.3) (Fig. 9). These corrections can be described by using extrapolation models[46] or pseudopotential models[31,47,56] up to[52,53] $\Gamma_D \sim 2-3$. To conclude this section of the paper we note that the applicability of the models discussed here is limited at low densities by the condition of local thermodynamic equilibrium (if this condition is not satisfied, kinetic models must be used to calculate the ionization of the plasma) and at high temperatures by the absence of data on the excitation energies and ionization potentials of multiply charged ions.

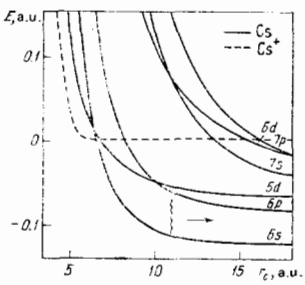

FIG. 6. Compression-induced changes in the energy spectrum of cesium. The wavy line shows the conditions of the experiments of Ref. 35.

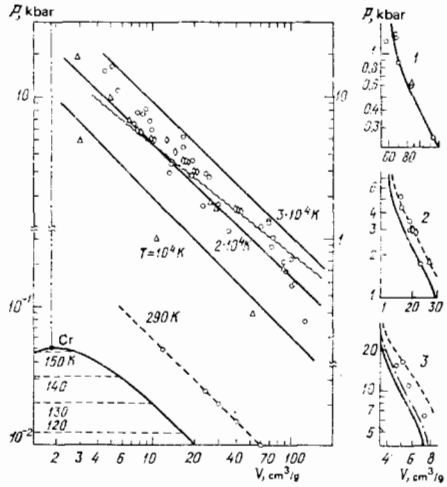

FIG. 7. Equation of state of an argon plasma.[52] Wavy line—Single-ionization boundary; points—experimental. The shock adiabatics were calculated from states with initial pressures $p_0 = 1$, 5, and 20 bar (curves 1, 2, and 3, respectively). Solid lines—Debye approximation; dashed lines—with distortion of the discrete spectrum according to the model of a bounded atom; dot-dashed lines—pseudopotential model.

4. QUASICLASSICAL MODEL OF MATTER

The description of the bound states of electrons at high densities $\rho \gtrsim \rho_0$ simplifies dramatically at ex-

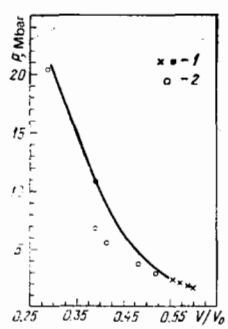

FIG. 8. Shock adiabatic of aluminum.[55] 1—Absolute measurements; 2—data from comparative measurements, found through the use of a smooth interpolation of the shock adiabatic of a reference (SiO_2) to calculations from the corrected Thomas-Fermi model.

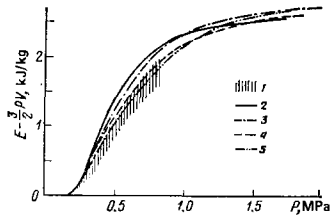

FIG. 9. Caloric equation of state of a cesium plasma[56] ($V=10^3$ cm^3/g). Γ_D—ratio of the Coulomb energy to the kinetic energy ("nonideality parameter"); α—degree of ionization; hatching—band of experimental errors; 1—Debye approximation in a grand canonical ensemble; 2—pseudopotential approximation; 3—asymptotic approximation taking the leading terms of the expansion into account; 4—approximation of an ideal plasma with atoms in the ground-state.

tremely high pressures, $P \gg e^2/a_0^4 \approx 300$ Mbar, or extremely high temperatures, $T \gg \mathrm{Ry} \approx 10^5$ K, where the electron shells are crushed, and their properties are described by the quasiclassical approximation of the self-consistent-field method: the Thomas-Fermi theory. In this model the description of the system in terms of wave functions and energy eigenvalues is replaced by a simplified statistical representation in terms of the average electron density $n(\mathbf{x})$, which satisfies the equations of a quasihomogeneous degenerate electron gas,[7]

$$n(\mathbf{x}) = \frac{1}{\sqrt{2}\pi} T^{3/2} f_{1/2}\left(\frac{p_F^2(\mathbf{x})}{2T}\right) \xrightarrow[T\to 0]{} \frac{p_F^3(\mathbf{x})}{3\pi^2},$$

where $f_{1/2}(\alpha)$ is defined in (3.2), and

$$\mu = \frac{p_F^2(\mathbf{x})}{2} + U(\mathbf{x}). \tag{4.1}$$

To simplify the calculations in the quasiclassical model, the substance is partitioned into electrically neutral spherical Wigner-Seitz cells containing a nucleus and the Z electrons surrounding it. It thus becomes possible to transform from a multicentered problem to a single-centered, spherically symmetric problem. The electrons are in a self-consistent potential $U(\mathbf{r})$ satisfying the Poisson equation

$$-\nabla^2 U = 4\pi n \qquad \left(U(\mathbf{r}) \underset{r\to 0}{\sim} \frac{1}{r},\ U(\mathbf{r}) \underset{r\to R}{\sim} (r-R)^2\right), \tag{4.2}$$

where the cell radius R is determined from the condition for electrical neutrality, $\int n(\mathbf{x})\, d\mathbf{x} = Z$. Through a numerical integration of (4.2) one can determine the electron density $n(\mathbf{x})$, which can then be used to construct all the thermodynamic functions of the electron gas of the atomic cell. To obtain the resultant thermodynamic characteristics of the model it is necessary to take into account, along with the electron terms, the motion of the nuclei, which is usually described in the ideal-gas approximation or the quasiharmonic approximation.[57] At $T \gg 10^7$ K and at solid-state densities, the contribution of the equilibrium radiation must also be taken into account. Equations (4.1)–(4.2) are self-similar in the nuclear charge: After the introduction of the variables

$$ZV,\quad Z^{-4/3}T,\quad Z^{-10/3}P,\quad Z^{-7/3}E;$$

they do not contain Z explicitly, and their solution applies to any element. This circumstance simplifies the use of numerical calculations using the Thomas-Fermi model.[58,59]

The Thomas-Fermi model is a quasiclassical limit with respect to the Hartree self-consistent-field equations, so that modifications of this model involve a more-detailed account of correlation, quantum-mechanical, and relativistic effects.[7] The correlation corrections result from the difference between the Hartree self-consistent field and the actual field in the atomic cell. These corrections result from the asymmetry of the electron wave functions and are interpreted as exchange correlation effects. Furthermore, because of the inaccuracy of the picture of independent particles adopted in the model, force-correlation effects appear.

Quantum-mechanical corrections arise because of the use of the quasiclassical formalism. These corrections can be said to consist of a part which is regular in terms of $\hbar^2$ (the so-called quantum part), which reflects the nonlocal coupling between $n(\mathbf{x})$ and the potential $U(\mathbf{x})$ due to the uncertainty principle, and an irregular part which reflects the nonmonotonic behavior of the physical quantities due to the discrete energy spectrum.[60] It is important to note that the introduction of an oscillatory correction is characteristic of the Thomas-Fermi model,[7] while the incorporation of exchange, correlation, and quantum corrections[59] is traditional for the physics of high energy densities. The relative magnitude of the correlation and quantum effects is determined by the dimensionless parameters[7] $\delta_{\mathrm{corr}} \sim \delta_0^{\nu}$ and $\delta_{\mathrm{qu}} \sim \delta_{\mathrm{ex}} \sim n/p_F^4$, which are given in the degeneracy region ($n^{2/3} \gg T$, $p_F \sim n^{1/3}$, $\delta_0 \sim n^{-1/3}$, $\nu = 2$) by $\delta_{\mathrm{corr}} \sim n^{-2/3}$ and $\delta_{\mathrm{ex}} \sim n^{-1/3}$ and in the classical region ($n^{2/3} \ll T$, $p_F \sim T^{1/2}$, $\delta_0 \sim n^{1/3}/T$, $\nu = 3/2$) by $\delta_{\mathrm{corr}} \sim n^{1/2}/T^{3/2}$, $\delta_{\mathrm{ex}} \sim n/T^2$.

A shortcoming of the Thomas-Fermi model is that it incorrectly describes the electron density at the periphery of the cell and near the nucleus, because of the violation of the quasiclassical conditions there. Kirzhnits[61] has proposed a method for resolving this problem through the use of successive approximations to solve the Thomas-Fermi equations with quantum corrections without a series expansion in a small parameter. This approach is the basis of the quantum-statistical model, in which the solution converges rapidly near the nucleus, while far from the nucleus the solution exhibits the correct quantum-mechanical behavior. The resulting expressions do not scale over Z, however: The numerical calculations must be repeated for each particular element. Furthermore, the equations themselves present far greater difficulties for numerical calculations. Several other modifications of the quasiclassical model near the nucleus have also been proposed.[7,62,63] They differ in the method used to make the corrections. In the thermodynamic description, however, the difference between these models and the corrected Thomas-Fermi model is significant only outside the region of their formal applicability, and for this reason the simple Thomas-Fermi model is preferred for specific calculations.

In using the quasiclassical description one should be clearly aware of the specific errors introduced by the cell model itself. In this model all the electron corre-

lations are automatically limited by the dimensions of the atomic cell, so they cannot exceed the average distance between nuclei, and there are no internuclear correlations. These circumstances impose an obvious limit on the applicability of the Thomas-Fermi model for describing plasmas under the conditions typical of this state, with the screening sphere including a significant number of nuclei, whose correlations with each other dominate the Debye correction.[64] Consequently, in contradiction of the assertion of Ref. 59, this model does not have the Debye limit in the plasma region. Furthermore, its extrapolation properties worsen with decreasing plasma density,[64] since the model does not reflect the stepped nature of the thermodynamic functions in a gaseous plasma (Fig. 10). Figure 13 (Section 5) also demonstrates the inadequacy of calculations by the Thomas-Fermi model and of the quantum-mechanical calculations from the Hartree-Fock-Slater model[65] in the characteristic plasma range.

Nuclear-correlation effects may also be important in a condensed phase, since the cell model ignores the deviation of the actual volume of the cells from the average volume (due to the motion of the nuclei). This approximation is valid only for ordered systems. At the values $\Gamma \sim 100$ characteristic of the condensed state and a dense plasma it is also necessary to incorporate in the equation of state the motion of the nuclei causing the fluctuations in the atomic volume. This effect was estimated for the Thomas-Fermi model in Ref. 66, where it was shown in the particular case of SiO_2 that the nuclear motion increases the pressure ~15% in the interval $1 < \Gamma < 100$.

The physical conditions for the applicability of the semiclassical model correspond to extremely high pressures, $P \gg 300$ Mbar, and extremely high temperatures, $T \gg 10^5$ K, which prevail in various astrophysical entities but which are still beyond the reach of our technical capabilities here on the earth. The highest pressures and temperatures which have been attained to data have been produced by dynamic methods using intense shock waves.[67-71] Although the data from shock-wave experiments do not correspond to the quantum-statistical conditions, they do give an idea of how well the quasiclassical models will extrapolate beyond their formal range of applicability, within which corresponding small parameters are in fact small.[67,72] The results of work along this line show that the quantum, exchange, and correlation corrections (the oscillatory corrections have not been considered) improve the extrapolation, making extrapolation possible, according to Al'tshuler *et al.*,[72] up to pressures $P \gtrsim 300$ Mbar at a zero temperature and up to ~50 Mbar at $T \gtrsim 10^5$ K. At the same time, the two possible interpretations[67,72] of the results of comparative measurements prevent an unambiguous answer to the question of which version of the quasiclassical model is preferable. These interpretations contradict the data from absolute measurements.[68,70] We might also note that recent experiments on the shock compression of highly porous copper at pressures of 10–20 Mbar and temperatures up to $2 \cdot 10^5$ K (Ref. 69) and of nonporous substances at pressures up to 160 Mbar (Ref. 71) point to significant shell effects in a region which has traditionally been described by the standard Thomas-Fermi model (see Fig. 11 and also Fig. 36 below).

Because of the initial simplifications, the quasiclassical model with the quantum and exchange corrections is not applicable at low pressures. Nevertheless, it does yield[59] a reasonable average of the atomic volumes of elements over the periodic table.[4)] We wish to emphasize that the Thomas-Fermi model itself leads to an infinite radius of the atomic cell at zero pressure because it lacks coupling forces; a finite density is achieved only by means of corrections. Kalitkin and Kuz'mina[59] have pointed out that the oscillations in the atomic volume fade with increasing pressure and approach the level predicted by calculations from the modified Thomas-Fermi models, although this effect can be credited in part to the circumstance that at high pressures the comparison has been made with the results of an extrapolation[74] of experimental data to the quasiclassical calculations themselves.

In fact, the tendency toward a simplification of the properties of a substance is disrupted at higher pressures because of the inner electron shells in the atom. It has been shown[7,60] that shell effects can be described qualitatively in the quasiclassical approximation by taking into account a correction which is irregular in $\hbar^2$ and corresponds to the oscillatory part of the electron density, previously (and erroneously) discarded. An important point here is that the shell effects are de-

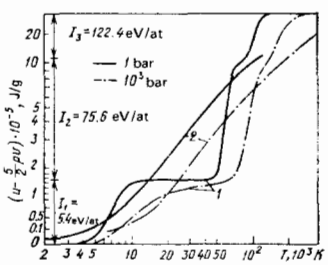

FIG. 10. Equation of state of lithium plasmas.[64] 1—Calculations from the chemical model; 2—from the Thomas-Fermi model with quantum and exchange corrections. I_1, I_2, I_3—successive ionization potentials.

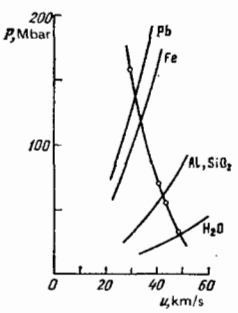

FIG. 11. Measurements of the relative compressibility of substances at ultrahigh pressures.[71] Points—Experimental; curves—calculations from the Thomas-Fermi model with corrections. The nonmonotonic deviation of the experimental data from the calculated results is evidence of significant shell effects.

scribed already in the lowest quasiclassical approximation for the wave function and must therefore be taken into account in addition to the corrections discussed above. According to Ref. 60, shell effects reflect irregularities in the properties of a substance caused by the discrete energy spectrum, and they arise in the quasiclassical model because of interference or de Broglie waves. The quasiclassical model in its most sophisticated version is thus quite a bit more meaningful than has been believed. It turns out that this model not only describes the average behavior of the electrons in heavy and highly compressed atoms but also reproduces qualitatively the inner shell structure of an atom[7] and frequently yields results in fair agreement with calculations using more-accurate quantum-mechanical models while being simpler and more graphic.

The shell effects significantly change the equation of state of a substance, causing discontinuities on the atomic-volume curve $V(Z)$ at high pressures (where this approximation is justified).[7] The equation of state acquires a characteristic nonmonotonic behavior, caused by the electronic phase transitions which occur as the energy levels are forced out of the discrete spectrum into the continuum. It might be expected that with increasing temperature this monotonic behavior would be smoothed out by resonance electrons. Nevertheless, results derived in the central field approximation[75] indicate (Fig. 12) that the shell structure is important even at an extremely high temperature. That shell effects are significant at hypermegabar pressures also follows from quantum-mechanical calculations in the Hartree-Fock-Slater approximation[76] (Section 5) and from calculations by the method of augmented plane waves[77] (see Figs. 14 and 15 below). These effects are predicted over broad ranges of the parameters[7] and should fade at $n \gg Z^4$ in the homogeneity region, as all the energy levels of the atom shift into the continuous spectrum. We might note in this connection that the asymptotic behavior of the quasiclassical model is not a trivial question, since it has been shown[78] that this model corresponds to the exact solution of the Schrödinger equation only in the limit $Z \to \infty$, but not in the limit of high densities.

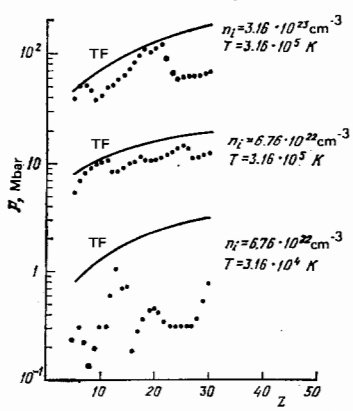

FIG. 12. Dependence of the pressure on the atomic number at a fixed density and a fixed temperature.[75] Solid curves—Calculations from the Thomas-Fermi model; points—calculations in the approximation of a central field with shell effects.

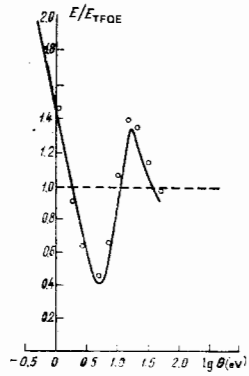

FIG. 13. Ratio of the energy of a lithium plasma according to the Hartree-Fock-Slater model[65] to the energy according to the TFQE model[59] at $P = 1$ kbar. The points are calculations from the chemical model.

In summary, the range of applicability of the quasiclassical model remains an open question to a large extent, and the behavior of substances at $P > 300$ Mbar is more varied than has previously been concluded from simple models.[58,59] An experimental test of the predictions of the quasiclassical shell model is the most interesting problem of the physics of ultrahigh pressures today. The solution of this problem will apparently require special experimental apparatus using high-power lasers,[79] electron beams,[18] or underground nuclear explosions.[68] Of significant interest in this connection is the reproduction of shell effects in the equation of state by means of direct quantum-mechanical methods; this topic is discussed in Section 5.

5. QUANTUM-MECHANICAL MODELS OF SOLIDS

At low pressures and temperatures, solids behave in a wide variety of ways. The various elements exhibit some very distinctive individual properties which can be explained on the basis of the particular electron energy spectrum of the atoms making up the crystal lattice. In this case the quantum-statistical description of Section 4, which averages the characteristic properties of the elements, is too crude, and direct quantum-mechanical methods must be used to calculate the thermo-

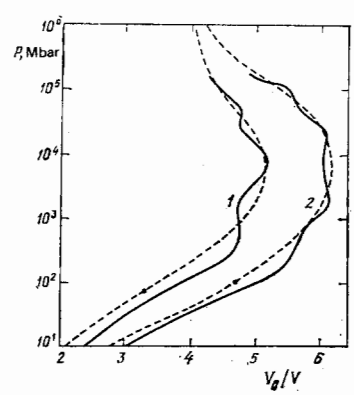

FIG. 14. Shock adiabatics of copper (1) and lead (2) (Ref. 76). Solid curves—Calculations from the Hartree-Fock-Slater model; dashed curves—calculations from the TFQE model and an interpolation.[72]

dynamic characteristics. Several methods have now been proposed for obtaining a quantum-mechanical description of the electronic, phonon, magnetic, optical, and other properties of the solids. The methods themselves have become highly refined. Here we will focus on the results calculated for the thermodynamic properties of substances over ranges of the pressure and the temperature as broad as possible. We will discuss only briefly the qualitative aspects of the methods, directing the reader to the original papers, monographs, and reviews for the details.[8,80-83]

In a thermodynamic description of a solid, one singles out the phonon and electron components,[8] which are studied independnetly, to a large extent. Most of the calculations on the electron spectrum have been carried out in a band model, in which the crystal is represented as an ideal periodic structure with fixed nuclei at the corners of cells, and each electron is moving in a self-consistent periodic potential produced by the ion lattice and the rest of the electrons. It thus becomes possible to express the wave function for the entire system in terms of one-electron Bloch functions.[80] The primary distinctions among the band-structure models lie in the methods used to calculate these one-electron functions within the elementary atomic cells into which the entire substance is partitioned and in the methods used to join the solutions at the boundaries.

With increasing compression, solids tend to convert into close-packed, highly symmetric crystalline structures, justifying the use of the Wigner-Seitz spherical-cell model in this case. According to this model, the overall self-consistent problem in the crystal is reduced to the solution of wave equation (3.11) in a single cell with Bloch boundary conditions,[80] under which the discrete energy spectrum of the free atom gives way to bands of allowed states. From the relationship between the pressure and the wave functions at the surface of the cell one determines the equation of state of the system.

Even simplified calculations in the spherical-cell model,[84] ignoring exchange effects [the term $G_{nl}(r)$ was omitted in (3.11)], have revealed the distinctive properties of the various elements, the structure of the electron energy bands, and the way in which these bands are filled. In contrast with the statistical model, the band theory reflects several qualitative effects of the periodic system, e.g., the different compressibilities and the normal density of neighboring elements in the periodic table. The distinctive ways in which the energy bands are filled cause irregularities in, and even a nonmonotonic behavior of, the pressure dependence of the properties of metals. The effect is seen in dynamic experiments as a change in the shock compressibility.[85]

When exchange effects are incorporated in a band model, serious calculation difficulties arise because of the need to solve a system of integrodifferential equations. An approximate way to incorporate exchange, with the real nonlocal exchange potential being replaced by an average local potential in the Hartree-Fock equations, was first proposed by Slater and has been developed further under the name of the "X– α method."[86] This method has been used to calculate the thermodynamic characteristics of the condensed phase of substances at high pressures and temperatures.[87] Nikifirovov *et al.*[65] have pursued the development of a method of this type for describing exchange effects, offering an expression for an effective exchange potential for arbitrary temperatures and densities.

Calculations using the Hartree-Fock-Slater model have demonstrated a much better agreement than the quasiclassical model with experimental data and the results of plasma calculations. All the results are characterized by oscillations with respect to the data of the quasiclassical models; the oscillations continue as long as there are shells in the system. It should be noted that the corrections for shell effects are also important where the exchange and quantum corrections to the Thomas-Fermi model are small. It can be seen from Fig. 13 that the energy of a lithium plasma at $T \approx 5$ and 16 eV is changed by a factor of more than two when shells are taken into account, although calculations by the Thomas-Fermi model and its modifications yield essentially identical results. Analogously, the shock adiabatics of copper and lead shown in Fig. 14 are quite different from the quantum-statistical results at pressures well above the traditional boundary estimate at 300 Mbar (Ref. 72), indicating that shell effects must be taken into account up to extremely high temperatures and pressures. It also follows from Fig. 14 that there is a sharp difference between the calculated and experimental shock adiabatics at low pressures ($P \leq 10$ Mbar), which indicates that the Hartree-Fock-Slater model is not accurate in this region.

The spherical-cell approximation is too crude for describing the properties of a solid under normal conditions, since the elementary cells of real crystals have much more complicated shapes, especially for structures with low coordination numbers. Furthermore, the relative importance of the exchange and correlation terms in the equation of state increases at low pressures, so that these terms must be taken into account more rigorously. A calculation of the intracell exchange interaction at $T = 0$ K and low compressions using the Hartree-Fock approximation and estimates of the correlation corrections and the intercell-exchange effects demonstrate that they strongly affect the calculated characteristics, casting doubt on spherical-approximation calculations in this region.[88] These circumstances have forced the development of effective new methods for self-consistent calculations for nonspherical structures at low pressures.

In real crystals the ions occupy a limited portion of the volume of an atomic cell, particularly at low degrees of compression. For a description of this situation, the crystal volume is partitioned into regions in which different methods are used to seek solutions of the Schrödinger equation. This partitioning makes it possible simultaneously to satisfy the boundary conditions at the surface of the elementary Wigner-Seitz cell, of complicated shape, and to take into account the difference between the lattice potential and the atomic

potential. The idea is to introduce a so-called muffin-tin potential,[86] which is spherically symmetric near the ion, where the wave function is a combination of the solutions of the Schrödinger equation in a central field, and constant in the volume between sites, with a solution in the form of a linear combination of plane waves. The two solutions are joined on a boundary sphere within the cell, with an augmented plane wave as a consequence.

Quantum-mechanical calculations by the method of augmented plane waves are more laborious than calculations in the spherical-cell model and have been carried out for the most part for structures under normal conditions; considerably fewer numerical results have been obtained for high pressures. Figure 15 compares the results calculated from this model[77] with the predictions of the quasiclassical approximations (Section 4) for aluminum. The characteristic deviations from a monotonic curve are caused by a transition of the L and K shells into the continuous spectrum at pressures of 50–750 and 10^4–10^6 Mbar. We see that the model of Ref. 77 predicts significant differences from the very simple versions of the quasiclassical approximation at pressures well above the boundaries estimated for the applicability of the Thomas-Fermi model in Ref. 72.

A combination of the method of augmented plane waves and the X–α method has been used[89] to determine the high-temperature equation of state of iodine and to study an isostructural phase transition in cesium. This method has been combined with a variational description of a liquid (Section 6) to calculate[90] the equation of state of condensed xenon. The critical volumes and pressures corresponding to the conversion of xenon into a metal upon compression were estimated ($V \approx 10$ cm^3/mole, $P \approx 1.5$ Mbar). The calculated results agree well with experimental results at low and high pressures, as can be seen (in particular) from Fig. 16, which shows the sensitivity of the course of the calculated shock adiabatic of xenon to different values of the conversion-to-metal volume. Some independent measurements of the optical absorption in condensed xenon were carried out recently in experiments involving compression using diamond anvils.[192] Interestingly, the

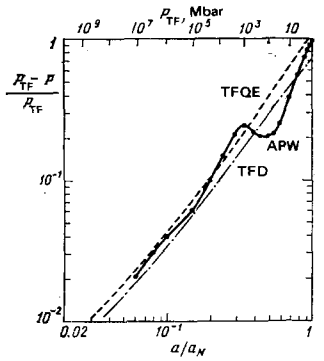

FIG. 15. Equation of state of aluminum[77] ($T = 0$ K). Calculations: TFD—Thomas-Fermi-Dirac model; TFQE—Thomas-Fermi model with quantum and exchange corrections; APW—model of augmented plane waves. Here a is the lattice constant.

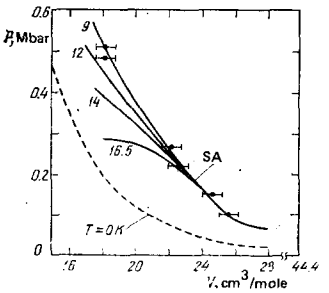

FIG. 16. Shock adiabatic (SA) and absolute-zero isotherm ($T = 0$ K) of condensed xenon.[90] The points are experimental. The curve labels are the volumes at which xenon becomes metallic upon compression.

volume dependence found for the width of the energy gap is also in approximate agreement with the calculated dependence,[90] and a conversion to metal is predicted at $P \sim 2$ Mbar.

The serious calculation difficulties which arise in the use of the method of augmented plane waves, especially at nonzero temperatures, has resulted in the widespread use in specific calculations of the method of linear muffin-tin orbitals, which, although slightly less accurate, permits much more rapid calculations.[91] This band-calculation method, which is usually employed for close-packed structures, takes the exchange-correlation effects into account in a self-consistent manner in the local-density approximation.[92] Over broad ranges of the pressure and the temperature, the linear muffin-tin-orbital method has yielded a quantitatively accurate description of the subtle characteristics of the Fermi surface which have been observed experimentally and also several features of the equations of state. These features are explained in terms of the sequence in which the electron energy bands are filled, for many metals. Although the method starts from first principles and employs no input parameters of any sort, it yields a very accurate description. For example, calculations of the normal density and the bulk modulus by this method have yielded results agreeing within 5% and 10%, respectively, with experiment.

The method of linear muffin-tin orbitals has been used to calculate the equations of state of lanthanum,[93] thorium,[94] calcium,[95] and silver.[96] The results agree well with data from static and dynamic experiments from normal conditions up to megabar pressures. Figure 17 compares the calculated $T = 0$ isotherm of calcium[95] with shock-wave data. In addition to giving a correct description of the equation of state, the calculation puts the transition of calcium into a semimetal in the same pressure range as is observed experimentally. This transition is explained as a change in the electron structure, which causes a sharp decrease in the state density on the Fermi surface at $V = 0.78V_0$; only an increase in the number of d states starting at compressions $V = 0.54V_0$ restores the metallic properties.

The use of this method to calculate the band structure at normal and elevated pressures has explained the redistribution of electrons and the changes in the nature of the electron states in cesium,[97] transition metals,[98]

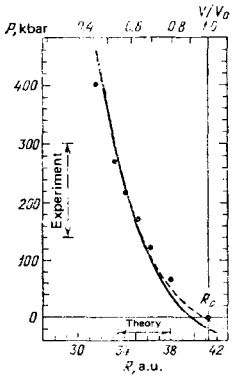

FIG. 17. Equation of state of calcium.[95] Points—Shockwave experiments; solid curve—calculated; dashed curve—with nonlocal corrections. The theoretical and experimental intervals ("theory" and "experiment") in which calcium converts into a semimetal are indicated.

the lanthanides,[93,99] and the actinides.[94,100] The thermodynamic consequences of these changes are discussed in detail in Section 6; at this point we will only show experimental data and calculated results[93] on the shock compression of lanthanum (Fig. 18), according to which the steep part of the shock adiabatic at $u \gtrsim 1$ km/s results from the completion of a 6s–5d electron transition.

All the calculations by the band-theory methods adopt the approximation of a static lattice, and significant difficulties accordingly arise in attempts to incorporate the vibrations of the crystal atoms in a self-consistent way. The effect of the temperature on the electron terms in the model is taken into account by averaging the calculated characteristics over a Fermi distribution.[89,93] The thermal contribution of the lattice atoms is determined from the cold curve[93,97] in the approximation of one of several quasiharmonic models which give a simplified description of the actual vibration spectrum. As a consequence, essentially insurmountable difficulties arise in attempts to use the cell model to describe the characteristics of a metal near the phase-transition curve (for lanthanium[93] and cesium[97]), where it is precisely the fine structure of the phonon spectrum which must be taken into account: the loss of stability of one of the vibration modes.

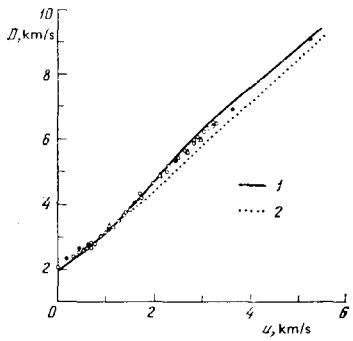

FIG. 18. Shock adiabatic of lanthanum.[93] 1—Calculated by the method of linear muffin-tin orbitals incorporating the 6s–5d electron transition; 2—calculation from the Mie-Grüneisen equation of state (γ/V = const); points—experimental.

In nontransition metals the ions occupy only a small fraction (~10%) of the volume of the atomic cell, and as the valence electrons move through the metal they spend only a small fraction of their time in the volume occupied by an ion. Since the properties of a metal are essentially independent of the particular behavior of the conduction electrons within the ion lattice, the actual potential of the interaction with the many-electron ion can be replaced by a simplified single-particle potential. A pseudopotential of this sort must conserve the scattering properties of the original ion, but the potential inside the ion can be much weaker than the actual potential. The introduction of a pseudopotential makes it possible to define a small parameter for the theory, U_k/ε_F (U_k is a Fourier component of the pseudopotential at the point of a reciprocal-lattice vector), so that perturbation theory can be used.[81] In the pseudopotential theory the metal is thus treated as a dense, degenerate plasma; the phonons are low-frequency collective excitations around the ground state, which corresponds to the regular positions of the ions.

The first successful quantitative descriptions of the properties of metals by means of pseudopotential models were achieved in a variety of single-particle approximations which reflect the many-particle nature of the problem in a nonsystematic way. Models of this sort have the shortcoming that they incorporate only the binary potential, ignoring the important indirect interaction of three and more ions through conduction electrons. A systematic pseudopotential theory incorporating the effective two-ion, three-ion, etc., interactions involves a rigorous series expansion in the electron-ion interaction parameter.[83] The many-particle formalism makes it possible to determine the dynamic characteristics of a metal—its phonon spectrum—at the same time as its static characteristics.

The use of this approach in the case of nontransition metals has yielded a consistent description of the phonon spectrum over the entire phase-volume region, the elastic constants, and the equation of state[83,101-103] (Fig. 19). This approach has also yielded energies and lattice constants and has made it possible to choose the most appropriate crystal structures and to analyze the effect of pressure on the lattice anharmonicity.[83,101] The pseudopotential method has proved to be particularly successful in calculating the equation of state of

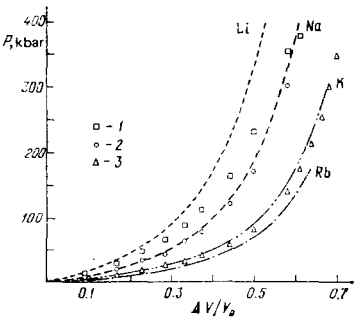

FIG. 19. Absolute-zero isotherms of the alkali metals.[101] The experimental points are plotted from the results of shock-wave measurements. 1—Li; 2—Na; 3—K.

metallic hydrogen,[104] whose ion has no electron shell, so that the calculations can be carried out to high degrees of compression. The thermodynamic characteristics of hydrogen have been calculated to terms of up to fourth order in the electron-ion interaction parameter. The equation of state has been found for all the structures competitive from the energy standpoint.

The use of the pseudopotential approach at high pressures is limited by the overlap of the ion cores and the lack of the necessary experimental data for constructing the pseudopotential of a compressed substance. According to Refs. 83 and 101, the upper limit on the applicability of the pseudopotential model for alkali and alkaline earth metals is of the order of hundreds of kilobars; below this limit the distortions of the pseudopotential are apparently of minor importance, and the effect of the compression reduces to simply changing the electron density.

The pseudopotential model was used in Ref. 105 to construct semiempirical equations of state for sodium and aluminum to describe the shock data at pressures up to ~1 Mbar. By fitting the parameters of the potential[106] it was found possible to calculate satisfactorily the shock compressibility of alkali halides outside the region of their polymorphic conversions. We might add that the equations of state found for ionic crystals in the quasiclassical approximation of the Hartree-Fock method and the shock adiatatics calculated from these equations of state[107] agree well with experimental data at pressures up to ~1 Mbar, above which the anharmonicity and thermal excitation of electrons become important.

6. MODELS FOR THE LIQUID STATE

With increasing temperature, phonon-phonon interactions become important in a solid and make the crystal lattice unstable with respect to the long-wavelength shear mode,[82] which causes the crystal to melt. The absence of a long-range order and the strong interparticle interaction severely hamper attempts to describe the liquid state theoretically. For a long time the liquid state has been regarded as a difficult problem and has been the least-developed branch of statistical physics. Attempts to extend to liquids ideas from the physics of gases have met with little success because of the sharp difference between the densities of the two phases (by two or three orders of magnitude), which mandates a large number of unknown virial coefficients in an expansion like (2.1). Even if the necessary coefficients could be calculated, the question of the convergence of series (2.1) at the densities corresponding to the liquid phase would remain open, since the existing proofs of the convergence of the virial series apply only to extremely low-density gases.[2]

The density of a liquid differs from that of a crystal by 10–20%, explaining the relative success in the use of solid-state approximations to describe liquids. The idea that liquid molecules are confined to a small volume by the average field exerted by their neighbors underlies the lattice model or the free-volume model.[108] This approach is of course most suitable for describing highly compressed liquids at low temperatures, at which the kinetic energy is only a small fraction of the total energy, i.e., under conditions which generally do not correspond to a liquid state. Consequently, the lattice model applies exclusively to states in the immediate vicinity of the melting curve; the melting is manifested by the formation of a multitude of defects in the crystal lattice, which is greatly distorted in the liquid state.[109]

Ideas from the solid-state and gas theories have been combined in the multiple-structure model,[108] according to which a real liquid is an equilibrium mixture of a gas and a solid, whose properties are described in terms of a binary distribution function or a partition function with an empirical parameter which performs the interpolation between a harmonic crystal and an ideal gas. Similar arguments are used in the cell model,[108] which partitions the entire liquid into molecular cells whose filling depends on the thermodynamic conditions. Models of this type furnish only a schematic description of the properties of a real liquid, but because of their simplicity they may be used effectively as elements of semiempirical models (Section 8). We might also note that the calculation methods of the cell model[110] have been refined to the point at which it is possible to find a consistent analytic description of the properties of solids and liquids and of the phenomenon of melting (Fig. 20).

Refinements in diffraction measurements[2] have yielded important information on the structure of liquids, which has improved our understanding of their properties. According to ideas based on experiments on the elastic scattering of x rays and thermal neutrons, there is a short-range order in a liquid which can be described by a binary distribution function $g(\mathbf{r})$, which determines all the equilibrium properties of the liquid state for a given interparticle interaction potential $\varphi(\mathbf{r})$. The statistical theory allows us to derive a relationship between these characteristics by working from nonlinear integral equations constructed on the basis of various hypotheses regarding the relative roles played by the short-range and long-range interactions in the system.[10-12] In turn, the Monte Carlo and molecular-dynamics methods make it possible to calculate $g(\mathbf{r})$ accurately for a given potential and to test the worth of the various integral equations.

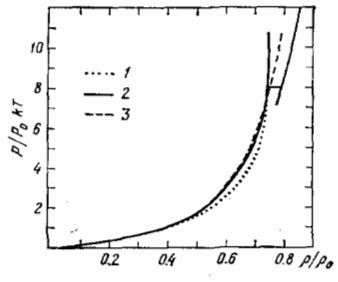

FIG. 20. Equation of state of a system of hard disks.[110] 1—Calculations from the self-consistent cell model; 2—calculations with cluster corrections; 3—Monte Carlo calculations.

The description of the liquid is thus determined by the choice of a suitable potential $\varphi(r)$; the quality of the approximations can be controlled experimentally, since the structure factor, i.e., the Fourier transform of the binary distribution function,

$$S(q) = 1 + n\int [g(r) - 1] e^{iqr}\, dr,$$

is an observable quantity in diffraction measurements. The description is closed, and it reduces to an analysis of how the properties of the potential affect the structural and equilibrium properties of the disordered system.

A governing circumstance in the development of new liquid models is the experimental fact that the structure of a liquid depends only slightly on the temperature at a fixed density.[2] In turn, the similarities among the structures of liquid metals, ionic systems, and dielectrics with very different attractive forces furnish evidence that these forces play only a minor role in shaping the equilibrium properties of liquids. These circumstances suggest that a repulsive potential is dominant, while the effect of the attractive forces and temperature effects in a dense liquid are at the level of corrections which can be dealt with by perturbation theory,[10] by a variational method,[111] or in the random phase approximation.[112]

In turn, for a model to describe the repulsive forces the simple potential of hard spheres of radius σ,

$$\varphi(r) = \begin{cases} \infty, & r \leqslant \sigma, \\ 0, & r > \sigma, \end{cases} \qquad (6.1)$$

is useful for describing the extreme state of a highly compressed, hot liquid. The hard-sphere model, the simplest nontrivial model of the liquid state, has won extreme popularity in the use of the integral-equation technique and numerical methods, and it has now been studied exhaustively.[10-12] Significantly, potential (6.1) has made it possible to derive an exact analytic solution of the Percus-Yevick equation, which is the best integral equation for describing a system with a short-range repulsion and which is used widely to calculate the properties of real liquids. The presence of a free parameter in the solution—the packing density $\eta = 4\pi\sigma^3 N/3V$—makes it possible to generate successfully descriptions of the structural characteristics of simple liquids and simple metals, by using various methods to determine this packing density.[10,12]

Calculations by various methods for systems with potential (6.1) have been carried out over the entire range of the liquid state. The best analytic description of the results is given by the Karnahan–Starling Pade approximation:

$$\frac{F_{HS}}{NkT} = \frac{4\eta - 3\eta^2}{(1-\eta)^2}.$$

Curiously, numerical calculations using the model (6.1) at densities approaching close packing of spheres, $\eta \lesssim 1$, have revealed structural anomalies and a tendency toward the appearance of long-range order in the system. This effect has been attributed[113] to crystallization of a geometric nature. We might note in this connection that most of the integral equations either fail to describe melting at all or predict it to occur at anomalously high densities.[2]

Further progress in the description of the properties of the liquid phase has been achieved through the use of the soft-sphere model, which uses a power-law repulsive potential

$$\varphi(r) = \begin{cases} \varepsilon(\sigma/r)^n, & r \leqslant \sigma, \\ 0, & r > \sigma. \end{cases} \qquad (6.2)$$

This model has also been used to calculate the equilibrium properties by the Monte Carlo and molecular-dynamics methods.[10,11,114] The results can be described approximately by

$$\frac{F_{SS} - F_0}{NkT} = \frac{1}{6}(n+4)\,\eta^{n/9}\left(\frac{\varepsilon'}{kT}\right)^{1/3},$$

where n is an additional adjustable parameter of the model. By analogy with the hard-sphere model, the power-law repulsive potential leads to melting,[114] with characteristics which depend strongly on n in this case. We might note in this connection that a numerical simulation of the properties of real systems by means of more complicated potentials such as the Lennard-Jones potential,[11] the stepped potential, and the square well[115] have provided melting and evaporation curves and a qualitative description of the isostructural electronic and polymorphic phase transitions in solids (Section 7).

The model of Ref. 116 for the liquid state combines the hard-sphere model (6.1) with the approximation of an average field. In this combined model the adjustable parameters are determined from the experimental sublimation energies and the experimental positions of the first peak in the structure factor of the liquid metal at the melting point. This model of the liquid state, like its predecessor, the van der Waals model, is a qualitative model, which does not give us a detailed description of the more subtle properties of a liquid. The agreement between theory and experiment can be improved substantially by appealing to the soft-sphere model, (6.2), and introducing some further adjustable parameters in the average-field model.[117,118] Figure 21 shows a representative result of this approximation[117]; here the parameters of the equation of state have been chosen from experimental results on the electrical explosion of uranium wires under pressure and the prop-

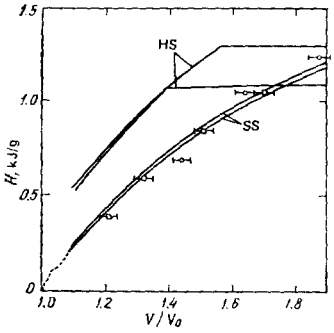

FIG. 21. Description of experiments on the electrical explosion of uranium wires under pressure by the hard-sphere model (HS) and the soft-sphere model (SS). Points—experimental; dashed curve—static data; solid curves—theoretical.

erties of uranium at standard pressure. The modified van der Waals models[116-118] are equally applicable for calculating the thermodynamic properties of dense gaseous phases, and they have an ideal-gas asymptotic behavior, so that they can be used successfully to construct wide-range semiempirical equations of state (Section 8).

Despite the extreme simplifications represented by the hard-sphere or soft-sphere model, they correctly incorporate the basic qualitative aspects of the many-particle interactions in a liquid, so they give a satisfactory description of the thermodynamic and structural properties of the liquid phase. These models can therefore be used as a zeroth-order approximation in a further perturbation-theory treatment[10-12] to take into account the details of the actual interparticle potential. A convenient calculation method for specific systems over a broad range of parameters, a method particularly effective in describing the properties of a dense liquid phase, is the perturbation-theory variational method,[111] which can determine the thermodynamic properties of a system with an arbitrary interaction potential through an average of the perturbation over the structural characteristics of the initial approximation, followed by a minimization with respect to its parameters.

A good zeroth-order approximation is the hard-sphere system, for which analytic expressions have been derived for the free energy and the binary distribution function,[12] so that explicit theoretical thermodynamic characteristics can be obtained for an arbitrary interparticle potential. The variational principle of a perturbation theory based on a hard-sphere system, which was the approach initially used to describe the properties of simple liquids under nearly critical conditions,[111] has been used for thermodynamic calculations of liquid simple metals and alloys,[9] single-component plasmas,[30] and dense, partially ionized plasmas.[119]

This description method has led to successful calculations of the characteristics of the liquid phase of metals over the range from standard pressure to states with a dense, fully ionized plasma; Fig. 22 shows some representative theoretical shock adiabatics of sodium and aluminum in comparison with the results of some shock-wave expreriments. The calculations by the variational method not only describe the experimental data but also agree well with the results of more-rigorous theoretical models at the extremely high pressures and temperatures which have not yet been studied experimentally.[119]

The method was subsequently generalized to use as a zeroth-order approximation the soft-sphere model, which is more realistic at high compression.[10] This approach has yielded successful descriptions of the properties of liquified gases: xenon,[90] argon,[121] hydrogen and deuterium,[122] and helium.[123] Variational calculations of the thermodynamic characteristics of the liquid phase of hydrogen, deuterium, and helium and the equation of state of the solid phase in the quasiharmonic approximation have revealed the positions of the melting curves of these elements.[122,123] Quantum-mechanical corrections were incorporated in the calculations in the liquid phase; anharmonicity effects were taken into account in the solid-state calculations. Figure 23 compares the calculated and experimental data in the liquid phase and on the melting curve for helium.[123] We see from this figure that the theoretical and experimental results agree well over the entire range studied. The accuracy of the description is similar in the cases of hydrogen and deuterium.[122]

The development of the variational method of perturbation theory for calculating the characteristics of liquid metals has led to the use as the initial approximation of the perturbation theory results obtained by the Monte Carlo method for a single-component plasma. Comparison of the calculations for the various versions of the variational method developed on the basis of systems of hard spheres or soft spheres or for a single-component plasma has shown[124] that the best description of the properties of lithium is found with the help of the characteristics of a single-component plasma. The results of a corresponding comparison[125] of the hard-sphere model and the single-component plasma as zeroth-order approximations in modeling the thermodynamics of liquid sodium and liquid aluminum show that the model of a single-component plasma is again preferable in the case of sodium, but for aluminum the hard-sphere model leads to a better agreement with experimental data (Fig. 24). This result is attributed to a greater rigidity of the ion core of aluminum, which is

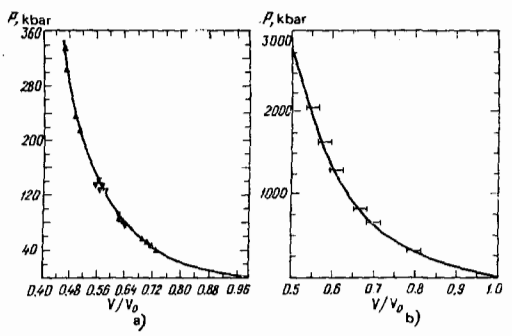

FIG. 22. Shock adiabatics of sodium (a) and aluminum (b).[119] Solid curves—Perturbation-theory variational-method calculations; points—experimental.

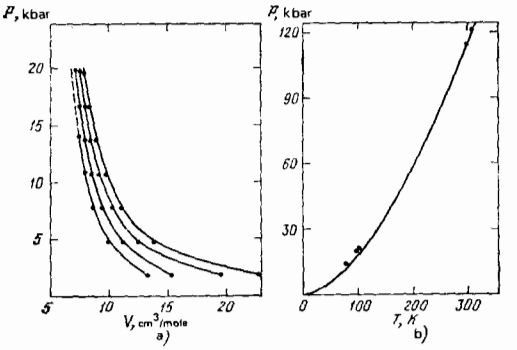

FIG. 23. a—Equation of state of the liquid phase of helium; b—melting curve of helium.[123] Experimental data are shown by the solid curves in part a and by the points in part b. The isotherm temperatures are 75, 150, 225, and 300 K.

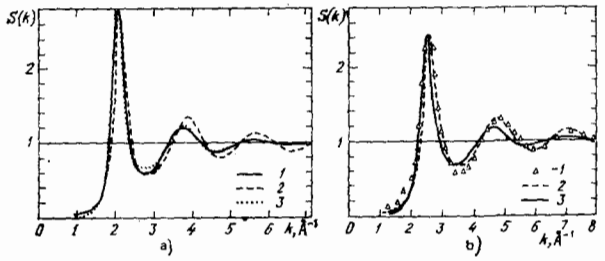

FIG. 24. Structure factors of liquid sodium (a) and liquid aluminum (b).[125] a: $T=373$ K. 1—Experimental data; 2—variational calculation from the hard-sphere model ($\eta=0.47$); 3—variational calculation from the model of a single-component plasma ($\Gamma=156$). b: $T=933$ K. 1—Experimental data; 2—hard-sphere model ($\eta=0.44$); 3—model of a single-component plasma ($\Gamma=119$).

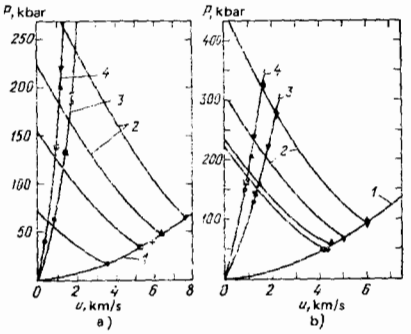

FIG. 25. Shock compression of liquid hydrogen (a) and liquid deuterium (b).[128] 1, 2—Calculations from the corrected hard-sphere model[126] for direct and reflected shock waves; 3, 4—shock adiabatics of reflecting magnesium and aluminum screens; points—experimental.

generally characteristic of polyvalent metals. Nevertheless, the results of Ref. 125 confirm that for systems with a soft repulsion (alkali metals, molten salts, and alloys) the model of a single-component plasma is preferable for use with the variational method of perturbation theory.

The use of perturbation theory to calculate the properties of a dense liquid phase is severely complicated by the nonadditivity of the interaction forces and the need to incorporate many-particle interactions. Since the interaction potential is usually not known accurately at the outset, a novel type of perturbation theory has been proposed by Kerley.[126] It uses as the zeroth-order approximation the cold curve for a solid, which effectively incorporates the nonadditive forces. The energy of the liquid is expressed in terms of variables characterizing the short-range order, and an average is taken over the cold curve furnished by experiment or by numerical calculations. The thermodynamic and structural characteristics of a liquid calculated from a corrected hard-sphere model[126] for various interaction potentials agree well with the results of Monte Carlo and molecular-dynamics calculations. The model has also proved to be effective for describing the thermodynamic properties of real liquids over broad ranges of parameters, and it yields results in agreement with experimental data at low[127] and high[128] pressures (Fig. 25). Curiously, the legitimacy of the approach of Ref. 126 has been confirmed independently by experimental results: The equations of state of the liquid and solid phases of alkali metals found from experimental data yield coincident ground-state curves.[129]

In addition to the direct problem of the statistical mechanics of a liquid—calculating its equilibrium properties from a given interparticle interaction potential $\varphi(\mathbf{r})$—the inverse problem has also received attention. In this approach, experimental data on the structure factor $S(\mathbf{q})$ are used to seek an appropriate potential.[12] The problem of finding the potential from diffraction measurements for inert gases and liquid metals is solved by the methods of molecular dynamics and integral equations; the integral approximation gives better results.[12] Analysis of the errors shows, however, that this inverse problem is an ill-conditioned problem: For a 10% accuracy in $\varphi(\mathbf{r})$, the initial experimental data on $S(\mathbf{q})$ must be accurate within 1%. To improve the accuracy in a search for the interparticle potential, additional information about the equation of state and the equilibrium properties of the liquid has been used in addition to the structure factor. The characteristics of the potential can also be found from thermodynamic information exclusively—without appealing to the data from diffraction measurements. Experiments on the shock compression of argon and on the scattering of molecular beams have,[121] for example, made it possible to choose the type of potential which gives the best description of the experimental data and to determine the parameters of this potential (Fig. 26).

7. PHASE TRANSITIONS

It is clear from the examination of the various models for a thermodynamic description of the properties of media that the ordinary classification of states frequently becomes indefinite and arbitrary at high pressures and temperatures, and the boundaries between phases either vanish completely or become indistinct, corresponding essentially to a continuous mutual transformation between adjacent states. In this section of the review we examine the relations between the different phases of a substance and thereby get a more defi-

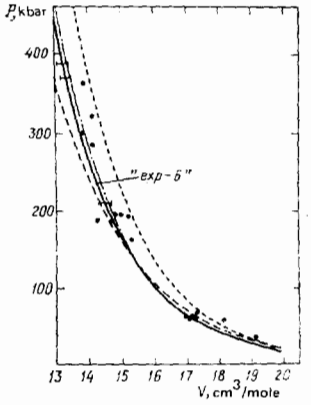

FIG. 26. Shock compression of liquid argon.[121] Points—Experimental; curves—shock adiabatics calculated with the help of various potentials (the best fit comes from the exp—6 potential).

nite picture of the general phase diagram with real and hypothetical phase transitions.

Melting is one of the most common and well-studied phase transitions, and since it is a transition from an ordered structure to a disordered one it involves the disappearance of long-range order from the system. A key question here is whether there is a type II critical point on the melting curve, at which a first-order phase transition gives way to a second-order transition, since Landau's results[130] indicate that the melting curve cannot terminate in a critical point. A necessary condition here is the simultaneous vanishing upon melting of the discontinuities in the volume, ΔV_m, and the entropy, ΔS_m, so that an experimental test of the theoretical predictions reduces to measuring these properties at high pressures.[13,131-133]

The experimental data presently available from temperature measurements at high pressures,[131] 0.5–3 Mbar, and volume measurements under static conditions[132,133] furnish evidence for the hypothesis that there are no type II critical points, since the discontinuities in the volume and entropy upon melting do not disappear with increasing pressure. Interestingly, the smallest measured values of ΔS_m have been greater than $R\ln 2$, i.e., greater than the lowest value associated with the disappearance of long-range order upon a transition from an ordered to a disordered structure.[13]

A detailed comparison of the available experimental data with the theoretical results obtained for certain simple systems (inert gases, single-component plasmas, charged spheres, and alkali metals) indicates that the structure dependence of the potential energy plays a leading role in melting.[13] In turn, this structure dependence depends only slightly on the particular nature of the intermolecular forces, and it can be described in the simple form in (6.1) or (6.2) for model systems. It is important to note that the data from these models also imply that there are no critical points, in accordance with the general conclusion.[130]

The Lindemann criterion is used widely for a quantitative description of the melting curve. According to this criterion, a solid melts when the amplitude (q) of the thermal vibrations of its lattice atoms constitutes a certain fraction A of the interatomic distance (R) in the crystal:

$$A^2=\frac{q^2}{R^2}=\frac{\langle E\omega^{-2}\rangle}{MR^2}, \tag{7.1}$$

where the average is taken over all the thermal vibration modes ω_i, and the energy of the i-th mode is given in the quasiharmonic approximation by

$$E_i=\frac{\hbar\omega_i}{e^{\hbar\omega_i/kT}-1}. \tag{7.2}$$

The actual spectrum of thermal vibrations and its volume dependence are usually exceedingly complicated, forcing us to appeal to models. For high-temperature melting, we have $E_i=kT$, and in the Debye approximation the conventional form of the Lindemann criterion follows from (7.1):

$$\frac{T_m}{\omega_D^2 V_m^{2/3}}=\text{const},$$

where ω_D is the Debye frequency. In the general case of an arbitrary spectrum,[82] we would have

$$\frac{d\ln T_m}{d\ln V_m}=2\left(\frac{\langle\gamma\omega^{-2}\rangle}{\langle\omega^{-2}\rangle}-\frac{1}{3}\right),\quad \gamma_i=-\frac{\partial\ln\omega_i}{\partial\ln V}, \tag{7.3}$$

and the usual assumptions adopted to simplify (7.3) are the condition

$$\langle\gamma\omega^{-2}\rangle=\langle\gamma\rangle\langle\omega^{-2}\rangle \tag{7.4}$$

and the replacement of the average value $\langle\gamma\rangle$ by the thermodynamic value: the Grüneisen coefficient $\gamma=V(\partial P/\partial E)_V$. The latter simplification is valid at high temperatures ($T>0.1\hbar\omega_D/k$). It follows from (7.3) that the melting temperature increases monotonically upon compression, since the experimental values of γ exceed 1/3.

Specific melting characteristics can be calculated with the help of (7.3) and (7.4) if we know the volume dependence of the Grüneisen coefficient, which is given in a generalized form[134] by

$$\gamma(V)=\frac{t-2}{3}-\frac{V}{2}\frac{(P_x V^{2t/3})''_{V^2}}{(P_x V^{2t/3})'_V}, \tag{7.5}$$

where $t=0$ corresponds to the Slater-Landau approximation, $t=1$ corresponds to the Dugdale-McDonald model, and $t=2$ corresponds to the Vashchenko-Zubarev free volume theory.[14] Here $P_x=P(V,T=0\text{ K})$ is the pressure on the absolute-zero isotherm. Methods for determining the parameter t in (7.5) and for finding the dependence $\gamma(V)$ from the data of static and dynamic experiments are discussed in Section 8. At this point we simply note that the optimum value of t may, in general, not be an integer; the melting curve of magnesium observed experimentally at high pressures,[135] for example, can be described with $t=0.55$ (Fig. 27).

The Simon and Krot-Kennedy melting laws which are used in practice[13] follow under specific assumptions from the Lindemann law. The generalization and reformulation of the criterion (7.1) for an arbitrary interparticle potential by the methods of statistical mechanics[136] provide further confirmation of this criterion. Monte Carlo calculations for a hard-sphere system[113] also demonstrate the validity of the Lindemann

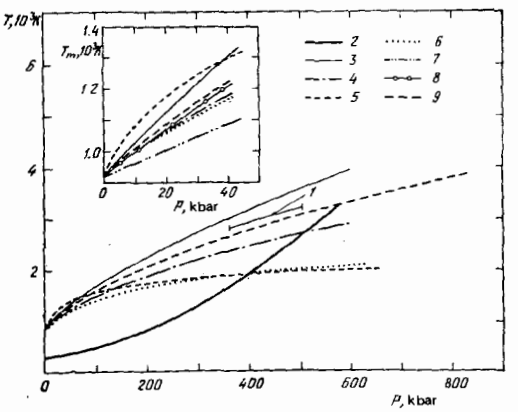

FIG. 27. Melting of magnesium during shock loading.[135] 1—Experimental; 2—shock adiabatic; 3, 4, 7, 9—calculations from Eq. (7.5) with $t=0$, 1, 2, and 0.55; 5—Simon law; 6—Krot-Kennedy law; 8—static data.

criterion for up to a doubling of the temperature and a quadrupling of the density; the melting sets in upon a 10% linear deviation from a close packing of the spheres. This criterion is based on simple physical considerations and has won much popularity in problems involving thermal and cold melting, in research on plasma crystallization, etc.

When the real vibration spectrum in a crystal is taken into account, we can also find from (7.3) a negative slope of the melting curve,[137] a consequence of the anomalous volume dependence of one of the long-wavelength vibration modes, which makes it possible to describe the nonmonotonic course of the melting curves. The experimental discovery of a softening of the transverse acoustic modes in the phonon spectrum of a bcc barium lattice under pressure, for example, has made it possible to explain the maximum on the melting curve on the basis of a decrease in the stability of this lattice.[138] The change in the nature of the interparticle interaction resulting from a change in the electronic structure may also contribute to the nonmonotonic behavior of the temperature on the melting curve, as has been observed for cesium and cerium.

The negative value of dT_m/dP_m can also be explained in the model of a two-component liquid,[139] according to which the liquid is a mixture of particles of two species, which are either formations with different coorindation numbers or atoms with an electronic transition which has already occurred (or without an electronic transition). The first case holds for substances which have loosely packed low-pressure phases; in this case the melting curve acquires a negative slope because of formations with the coordination numbers of the high-pressure phase near the phase boundary. This interpretation is supported by an analysis of the structural data, which indicates the presence (in the cases of Hg and Sn) or in fact a dominant role (in the cases of Bi, Sb, and Ga) of formations of the high-pressure phase in a liquid near the melting curve.[139]

There is a different situation in the melting of metals which permit (as the lanthanides do, for example) a possible change in the electronic structure. The slope changes and the pronounced decrease in the compressibility observed experimentally on the shock adiabatics of the rare earths[140-142] have been attributed to a completion of electronic transitions[85,140] or to a high rigidity of the filled $5p^6$ inner shell of xenon.[141] As Grover and Alder were the first to point out,[143] the experimental slope changes on the shock adiabatics of the lanthanides usually occur on the parts of the melting curves extrapolated from low pressures. The pronounced size of these slope changes is evidence for large negative values of dT_m/dP_m at the intersection of the two-phase region.

Careful measurements of the shock adiabatics of the lanthanides[142] have made it possible to work from the shock-wave and static data to plot melting curves up to high pressures ($P \lesssim 1$ Mbar) and to determine the points at which these curves intersect the adiabatics. These intersection points coincide quite clearly with the experimental slope change for all metals (Fig. 28). Since

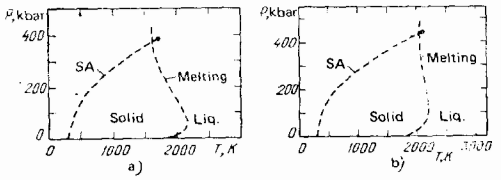

FIG. 28. Phase diagrams of thulium (a) and erbium (b).[142] Dashed curves—Calculated temperatures on the shock adiabatic (SA) and the melting curve (melting); points—melting on the shock adiabatic according to experimental data.

the high-pressure phases of the rare earth elements are extremely closely packed, the anomalous behavior observed on the melting curves and thus the higher density of the liquid cannot be attributed to the presence of higher coordination numbers in the liquid. Working in the model of a two-component liquid, we conclude that a continuous change in the electronic structure which tends to increase the density occurs in the atoms of a liquid as the pressure is raised. In the solid phase, the change in the electronic structure either also occurs continuously (as in the case of cerium), but at a different rate, or begins at the triple point (as in the case of cesium), giving rise to anomalies on the melting curves of the lanthanides.

The specific mechanism for the change in the structure which increases the density and reduces the compressibility can be different in different cases; it has been interpreted as either the completion of s–d electron transitions and the formation of relatively incompressible shells (in the case of lathanum[93]) or a sharp decrease in the metallic radius of the ion upon a delocalization of f electrons (cerium[99] and praseodymium[144]). We wish to emphasize that the correspondence between the position of the slope changes on the shock adiabatics of the lantanides and the intersection of these adiabatics with the melting curves is not absolutely necessary; the slope change (or a sharp bend[93]; see Fig. 18) due to a redistribution of electrons can also occur in the solid phase. In the lanthanides, however, this correspondence is quite convincing because of the anomalous melting curves and the low temperatures on them and also because of the substantial pressures corresponding to the change in the electronic structure. We apparently have a situation of a different type in the cases of the refractory metals (Ti, Zr, Hf), where the completion of the s–d transitions on the shock adiabatic occurs in the solid phase and is accompanied by structural phase transitions.

A maximum also appears on the melting curve at extremely high pressures because of quantum effects.[21] As a crystal is compressed, the spatial localization of its nuclei increases the uncertainty in the momentum and thus increases the amplitude of the zero-point vibrations. The energy of these vibrations, $\hbar\omega_D \sim \hbar\omega_0 \sim n^{1/2}$ (ω_D and ω_0 are the Debye and plasma frequencies of the ions), increases more rapidly with increasing density than the Coulomb energy, $\sim n^{1/3}$, which tends to stabilize the lattice. The ultimate result is a melting of the crystal at $T = 0$ K; i.e., the region occupied by a crystalline state is bounded. Estimates of the limiting

densities of crystals are afflicted by extremely large uncertainties, but at any rate these densities lie in the range[21,36] $\rho \sim 10^3-10^8$ g/cm^3.

At pressures of hundreds of kilobars, solids can have different crystal structures, depending on the thermodynamic conditions. Transitions between different structures give rise to additional phase boundaries. The classification and description of polymorphic phase transitions constitute a complicated and laborious problem, requiring accurate calculations of the energy and phonon spectra of the competing modifications. As a result, the primary source of information about polymorphic transitions has been direct experiment, static and dynamic.[145] A general tendency in the phase transitions is a pressure-induced transition of a crystalline substance into more closely packed structures with maximum coordination numbers. According to dynamic measurements,[146,147] the polymorphic phase transitions are completed at 0.5–1 Mbar.

The qualitative features of the phase diagram of various substances, with allowance for the polymorphic transitions between different close-packing versions, have been reproduced successfully in molecular-dynamics calculations using a square-well potential[115] corresponding to an effective attraction between the atoms and the crystal lattice (Fig. 29). Calculations with a stepped potential[115] simulating change in the ionic radius have explained details of isostructural conversions in metals and have revealed anomalous types of phase transitions which are characteristic of cesium and cerium.

In a compressed substance, there are also electronic phase transitions (predicted some time ago by Fermi) which do not directly involve a change in the symmetry of the crystal lattice and are instead caused by a change in the electronic structure of the elements. The most representative conversions are those observed in the metals of the long periods, which exhibit an inversion in the filling of their energy levels. As the pressure is raised, the electrons become redistributed among shells, and this inversion is progressively eliminated, changing the binding energy of the crystal and giving rise to structural phase transitions.

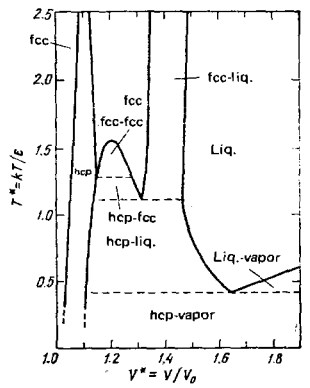

FIG. 29. P–V phase plane of a system of particles with a square-well interaction potential.[115] The polymorphic modifications of the solid phase have fcc and hcp lattices. An interesting isostructural hcp-hcp transition with a critical point has been observed experimentally in cerium.

The factor primarily determining the particular type of crystal lattice in a metal is the number of binding d electrons. As was shown by the calculations of Ref. 148, the s–d transition and the increase in the population of the d band upon the compression of transition metals and even simple metals are primarily responsible for the observed sequence of phases in these elements. Corresponding calculations of the binding energy of various structures in the trivalent lanthanides[149] have revealed a correspondence between the optimum lattice type predicted by the calculations and the lattice type observed experimentally as the number of d electrons is increased upon compression from 1.5 to 2.7; absolutely no role is played in the process by a redistribution of f electrons. Further evidence that the trivalent lanthanides behave in the same manner as transition metals upon moderate changes in volume comes from the experimental observation of the sequence of phases characteristic of the transition metals in yttrium,[150] which lies in the same group, III, but which does not contain f electrons.

The picture of events was marred by an unexpected result: the appearance at high pressures of the rare crystal lattice corresponding to the β phase of neptunium in scandium, which is the first transition metal in group III (Ref. 193). This result indicates, first, that the approximate band calculations of Refs. 148 and 149, which ignore the hybridization of the s–d bands (which gives rise to this rare lattice), are inadequate in this case; second, it indicates that the 5f electrons have only a minor effect on the binding energy of the actinides, since structures similar to the neptunium β phase are customary for them. Syassen *et al.*[196] recently carried out a very interesting study of the structure of the lanthanides at high static pressures ($P \lesssim 500$ kbar). They found that the sequence of structural first-order phase transitions which leads to the closest-packed fcc lattice becomes supplemented at higher pressures by a second-order phase transition, which involves a growing distortion of the fcc structure and which results from a complex hybridization of bands at high degrees of compression. This transition is further evidence that the single-particle calculations[148,149] are of limited applicability under these conditions. Some unusual properties are exhibited by the electronic transitions in the lanthanides which involve a displacement into the conduction band of some narrow, essentially localized, f bands. An electronic transition of this sort, from a localized level to a collectivized state, is accompanied by the phenomenon of an intermediate valence[197]: Each atom has a nonintegral number of conduction electrons. An element which exhibits this type of transition is ytterbium. As ytterbium is compressed from 40 to 300 kbar, one observes,[198] without a change in crystal structure, a continuous increase in the number of valence electrons from 2 to 3, with a corresponding change in the electronic structure from the $4f^{14}(5d6s)^2$ state to the $4f^{13}(5d6s)^3$ state. Incidentally, there is the possibility that this transition is related to the delocalization process discussed below.

Electronic phase transitions are not necessarily

linked to changes in the symmetry of the crystal lattice; furthermore, they occur in both the solid and liquid phases. The most characteristic example is the Mott transition, which corresponds to a delocalization of electronic shells upon compression. In this case the populations of the levels change only slightly, but at a critical compression the nature of the electronic states changes, and an electronic shell becomes a conduction band. The Mott transition can occur without a structural change, and it terminates in a critical point; on this basis it may be regarded as a phase transition between a gas and an "electronic liquid."[151]

The metal exhibiting this transition which has received the most experimental study is cerium,[145] in which the delocalization of a 4f electron upon compression at a modest temperature causes a significant (~15%) decrease in the size of the ion, which in turn causes an isostructural phase transition with a critical point. The element following cerium in the lanthanide series, praseodymium exhibits at ~200 kbar a structural phase transition between similar close packings[144] which involves a delocalization of 4f electrons. This transition is also accompanied by a sharp decrease (~19%) in the metallic radius of the ion. These examples both support the explanation of the anomalous melting curves of the lanthanides by the model of a two-component liquid (more on this below), and they imply a greater degree of collectivization of the f electrons in the liquid phase, which increases the density and reduces the compressibility upon melting.

In metals, the effects of a change in electronic structure or of a delocalization of shells are seen both in dynamic experiments, in a decrease in the compressibility of the new phase,[140-142] and in static experiments, in discontinuities in the resistivity[152] and changes in the structural characteristics of the crystal.[145] Electronic phase transitions have also been the subject of extensive theoretical study[84,93-100] by band-theory methods (Section 5). The calculated results have furnished a correct explanation for the experimentally observed effects, and they have confirmed the general trend in the pressure-induced changes in the electronic structure toward a hydrogen-like arrangement of levels. Band-structure calculations carried out for lanthanum by the method of linear muffin-tin orbitals,[93] for example, have demonstrated a 6f–5d electronic transition and a quantitative agreement between the point at which this transition is completed and the point at which the decrease in the shock compressibility is found experimentally (Fig. 18). It turns out that a temperature increase smooths out the transition effects by virtue of a broadening of the energy bands. The particular electronic characteristics of metals near the singular point of an electronic transition caused by a pressure-induced change in the topology of the Fermi surface have also been studied.

An interesting theoretical result is the description of the delocalization of f electrons upon the compression of the lanthanides and actinides. Calculations for cerium[99] show that the 4f band contracts upon a decrease in the density and splits into two states corresponding to different spin polarizations. The effect corresponds to a transition of a 4f electron from a metallic state to a localized state, and it can be linked with a $\gamma-\alpha$ transition, which is accompanied by the appearance of antiferromagnetism in the γ phase and which has been studied experimentally in some detail.[145] We wish to emphasize that at low temperatures this transition is a purely Mott transition, not an f–d transition, since the calculations of Ref. 199 show that in the α phase the $4f^1(5d6s)^3$ electronic configuration is preferable to the $(5d6s)^4$ transition from the energy standpoint; furthermore, the former transition leads to a much better agreement between the theoretical and experimental transition energy and bulk modulus. Above the critical temperature, however, the difference between the delocalization of an f electron and an f–d electronic transition apparently becomes quite arbitrary. Calculations by the method if linear muffin-tin orbitals have also provided a quantitative description of the abrupt changes in the magnetic properties of transition metals at temperatures above the Curie point. The effect has been attributed to a preference for states with unpolarized spin at the transition, because of a decrease in the energy.[98]

A delocalization of f electrons can occur not only upon compression, as is observed in the cases of cerium and praseodymium, but also as a function of the atomic number, as can be seen in the actinide series. Figure 30 shows experimental and theoretical values of the equilibrium atomic radii of the actinides.[100] There is a complete agreement between the experimental and theoretical results for the first few elements of the series, but the agreement is disrupted at neptunium and plutonium. Correlation effects become more important for these elements, and at even a slight negative pressure a solution with a polarized spin becomes preferred; for americium, this solution is also the optimum solution under standard conditions. Americium is therefore the first element in the actinide series which has localized 5f electrons and which exhibits the characteristic properties of the rare-earth elements. Calculations[100] have shown that there should be a delocalization of 5f electrons, accompanied by a decrease in the metallic radius, when americium is compressed, by analogy with cerium and praseodymium. Interestingly, this prediction has been confirmed experimen-

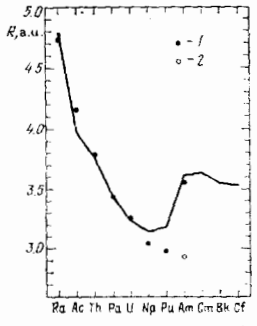

FIG. 30. Experimental and theoretical (1) atomic radii of the actinides.[100] 2—Theoretical value calculated for americium without allowance for localization of 5f electrons.

tally[154]; although the change in volume at the transition has turned out to be lower than that predicted theoretically,[100] the high-pressure phase has the low-symmetry structure of the uranium α phase, which is also observed in the α' phase of cerium. The actinides coming after americium will presumably also undergo compression-induced transitions to the exotic structures with low coordination numbers which are characteristic of the first few elements of the series.

Temperature, like pressure, can strongly affect the nature of the f-electron states. Under standard conditions, plutonium and neptumium have delocalized 5f electrons, but even a slight increase in the volume is accompanied by a transition of these electrons to a localized state.[100] In a study including the anomalously high volume expansion coefficient of plutonium and neptunium and the definite role played by the hybridization of s–d bands in the formation of the neptunium β phase,[193] Vohra and Holzapfel[194] concluded that a localization of 5f electrons occurs in the high-temperature solid phases of these metals and explains the observed anomalies in their properties.

Electronic phase transitions also result from a compression-induced shift of inner electron shells from the discrete spectrum into the continuum. According to Kirzhnits and Shpatakovskaya,[60] this effect corresponds to a first-order phase transition. An electronic phase transition of this sort is of course the end result of a succession of phase transitions which amount to a pressure-induced ionization of a sequence of electron shells. The parameters of these phase transitions calculated by the semiclassical theory (Section 4) and by direct quantum-mechanical methods (Section 5) correspond to pressures well above 300 Mbar, making it difficult to test these predictions experimentally. It may be that these transitions are responsible for the anomalous features observed on the mass-radius curves of white dwarfs.[60]

Some interesting features are observed by phase transitions in disordered structures, where a competition between attractive and repulsive forces in the interparticle interaction gives rise to a liquid-vapor transition which terminates in a critical point. The characteristics of the boiling curves and the parameters of the critical points have been measured for a large number of chemical compounds and can be found in the voluminous handbooks. Particularly thorough experiments have been carried out in the critical region, where the data on the critical indices, the spatial and temporal fluctuations, the kinetic coefficients, etc., have served as a foundation for the construction of the various theories of critical phenomena.[2] The information available on the positions of the boiling curves of most of the chemical elements is, however, quite limited. For example, among the metals, which make up about 80% of the elements in the periodic table, the parameters of the critical point have been determined for only three, the lowest-boiling metals,[155] and the situation is even sadder when we start looking for detailed studies of the phase boundary or of near-critical and, especially, supercritical states.

The parameters of the critical points of elements can be estimated from the tabulated heats, temperatures, and densities on the liquid-vapor equilibrium line through the use of the thermodynamic analogies in their properties (Fig. 31). The thermodynamic scaling principles and the parameters of the critical points of most elements which have been found by various methods are given in Refs. 155 and 156. On the whole, the results found by the different methods are not far apart, although the quantitative differences in the critical parameters sometimes reach 30–50%. Similar results are also found from model equations of state (see Fig. 36, somewhat below) and are supported independently by experimental data on the adiabatic expansion of shock-compressed metals[157] and on the slow electrical explosions of metal wires.[117,118,158]

An important feature of the evaporation of metals is that the high-temperature part of the boiling curve is in the plasma phase because of the high critical temperatures, which are comparable to the corresponding ionization potentials. Because of the high critical densities, this plasma phase is very nonideal with respect to a broad spectrum of interparticle interactions. The evaporation of metals at high pressures thus occurs directly to a plasma phase, skipping the gaseous region, in contrast with the events in the case of low-boiling substances. The effect may distort the estimates of the boiling phase boundary and may also give rise to new phase boundaries.

As mentioned in Section 3, several qualitative descriptions of the physical properties of nonideal plasmas have been generated from heuristic models based on the extrapolation of arguments regarding collective and quantum effects with a Coulomb interaction from the region of slightly nonideal plasmas. Typically, some of these models lose their thermodynamic stability at high ratios of the Coulomb energy to the kinetic energy, and the effect has been linked[4,5,35] to the possibility of a first-order phase transition and to a stratification of a highly compressed Coulomb system into phases with different densities.[159] It may be that the experimental anomalies observed in the dielectric permittivity of mercury vapor[195] are evidence of precisely this stratification, into a weakly ionized gas and a

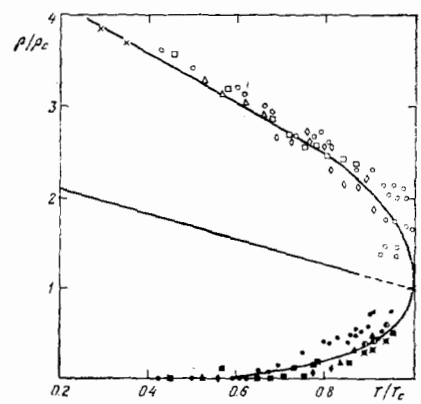

FIG. 31. Curve of the coexistence of the liquid and vapor of alkali metals.[155]

charged, relatively dense, disperse system. The triple point on the liquid-vapor equilibrium line corresponds in this case to a Mott metal-dielectric transition in the liquid phase.

Several studies have been carried out to determine the expected properties of nondegenerate, highly nonideal plasmas and the characteristics of the phase transitions in them. The many possibilities here have been analyzed by means of simple models[4] and by pseudopotential calculations by the Monte Carlo method.[47] The primary effect, which causes the condensation of a multicomponent plasma, is the polarization attraction of unlike charges. In this case the stabilization of the dense phase is attributed to quantum effects (interference) or, at high densities, to degeneracy and overlap of the electron shells of atoms and ions. Another possibility which has been discussed recently is a phase transition in a weakly ionized dense plasma caused by an interaction of charges with neutrals.[49]

The model-based analysis of highly compressed Coulomb systems predicts a possible formation of a Wigner electronic crystal, which has become the subject of a fair number of theoretical papers[35] and experimental searches[40,41] (Section 3). Landau and Zel'dovich[160] discussed the possibility of anomalies in the thermodynamic functions upon the transition of a dense metal vapor to a metallic state. They predicted that phase transitions in the gas and liquid phases other than the boiling curve of the ordinary type might be caused by the conversion to a metallic state.

The theoretically predicted plasma phase transitions would greatly distort the customary phase diagram of a substance, giving rise to additional phase boundaries and to exotic plasma phases. The heutristic models, which clearly are no more than qualitative models, suffer from large uncertainties in their conclusions. The conclusions depend on the particular ways used to describe plasmas with parameters in the very nonideal region. In particular, since phase transitions are predicted for plasma states with a strong interparticle interaction, where the theory is most uncertain, a final resolution of the question of whether the specific plasma phases exist must await experimental data. The quantitative data presently available on the properties of nonideal plasmas from dynamic experiments[52,53,118,157,158] do not show any definite indications of a significant phase stratification, and they suggest that the phase diagrams of the substances which have been studied are of the usual form, with a single critical point (Fig. 1). To conclude this section we wish to emphasize that the existence of specific phase transitions is a hypothetical possibility but an extremely interesting one from the standpoint of experimental high-temperature thermophysics.

8. SEMIEMPIRICAL EQUATIONS OF STATE

It follows from the preceding sections that a description of the thermodynamic properties of nonideal media requires complex models which are tailored to fit a particular situation and are accordingly applicable only in a limited region of parameters. These models usually require extensive numerical calculations, and the results are in the form of graphs or tables of limited size, making the results difficult to use for practical calculations.

An alternative method for describing the properties of nonideal media over a broad region of parameters is to construct semiempirical models[14-16] in which the general functional dependences are found from theoretical considerations, while experimental data are used to determine the numerical values of the coefficients in these functions.[5)] The most common approach in the semiempirical models has been to divide some thermodynamic potential (the free energy, for example) into a cold component $E_{cold}(V)$ and thermal components determined by thermal excitation. These thermal components are written in turn as the sums of the contributions of the thermal motion of the atoms or molecules of the crystal lattice, $F_{latt}(V,T)$, and the contribution of the thermally excited conduction electrons, $F_e(V,T)$:

$$F(V, T) = E_{cold}(V) + F_{latt}(V, T) + F_e(V, T), \qquad (8.1)$$

where the particular nature and form of the various terms depend on how general the corresponding semiempirical models are.

The relatively low temperatures in dynamic compression to pressures of hundreds of kilobars allow this part of the quasiharmonic model (7.2) to be described successfully in the form of a Mie-Grüneisen equation of state,

$$P(V, E) = P_{cold}(V) + \frac{\gamma(V)}{V}[E - E_{cold}(V)], \qquad (8.2)$$

where the relationship between $\gamma(V)$ and the cold curve is determined from (7.5). The experimental fact[15,18] that the wave and mass velocities are related linearly, $D = C_0 + \lambda u$, leads to the following equation for the shock adiabatic:

$$P(V) \quad \frac{C_0^2(V_0 - V)}{(V_0 - \lambda(V_0 - V))^2}.$$

The procedure of Refs. 14 and 18, which incorporates the third-order tangency of the shock adiabatic and the absolute-zero isentrope, can therefore be used to construct an approximate relationship between the parameter t in (7.5) and experimental results: the Grüneisen coefficient $\gamma_0 = \gamma(V_0)$ and the slope of the adiabatic, λ:

$$\gamma_0 = 2\lambda - \frac{2+t}{3}.$$

There are many other possible ways for determining t from static and dynamic measurements.[164] Comparison of the various calculations of $\gamma(V)$ with experimental data on aluminum[165] shows, however, that none of the quasiharmonic models has any decisive advantage in describing the dynamic experiments.[164] Equally unsatisfactory results are found in a comparison with the data of Ref. 165 of the highly simple approximation γ/V = const, which is the approximation most commonly used in calculations.[6)] We might also note that the use of Eq. (7.5) to calculate $\gamma(V)$ is, strictly speaking, legitimate only for isotropic structures or structures of cubic symmetry. In general, the tensor nature of the Grüneisen coefficient must be taken into account. De-

lannoy and Perrin[167] have discussed a method for determining the Grüneisen coefficient from measurements of the elastic constants and their derivatives with respect to the pressure for several metals of cubic and hexagonal symmetry. We wish to emphasize again that a complete solution of the problem of the behavior $\gamma(V)$ can be found only by taking into account the actual spectrum of vibrational frequencies in the crystal (Section 7).

The Mie-Grüneisen equation of state (8.2), which describes the properties of solids at relatively low temperatures, contains the two unknown functions $P_{\text{cold}}(V)$ and $\gamma(V)$, which are related by differential equation (7.5). In practice, however, the solution of this equation does not make it possible to find unambiguously the density dependence of the Grüneisen coefficient, since the derivatives of P_{cold} required in the calculation are determined from the experimental shock adiabatic at a severe cost in accuracy. Various analytic expressions which give identically good descriptions of the raw data from the shock-wave experiments predict qualitatively different types of $\gamma(V)$ behavior.[168]

An alternative way to describe shock-wave experiments and to extract equations of state is to specify the cold curve analytically and use several adjustable parameters.[168,169] A convenient way to represent P_{cold} is a series expansion in the cubic root of the compression,[168] $\sigma_k^{1/3}$ ($\sigma_k = V(P=0, T=0)/V$)[168]:

$$P_{\text{cold}}(\sigma_k) = \sum_{i=1}^{7} a_i \sigma_k^{1+(i/3)}, \tag{8.3}$$

where the coefficients a_i are found from experimental data on the compressibility, the Grüneisen coefficient, and the sublimation energy under standard conditions and from calculations from quantum-statistical models and the parameters of a single experimental point on the shock adiabatic. The approximation

$$P_{\text{cold}}(\sigma_k) = Q\{\sigma_k^{2/3} \exp[q(1-\sigma_k^{1/3})] - \sigma_k^{4/3}\},$$

which follows from the theory of ionic crystals, has been used to find equations of state of several metals.[169] A similar expression for P_{cold} has been used to derive equations of state for many metals and minerals.[16]

The approximate expressions derived for the cold curve in this way give a reliable description of this curve at pressures up to ~10^3 Mbar, but they do not exhibit the correct quantum-statistical asymptote in the high-density limit. Expressions of the type in (8.3), but with lower powers, have been proposed[74] for calculations at extremely high pressures. The higher-order terms (~$\sigma_k^{5/3}$ and $\sigma_k^{4/3}$) have the exact quantum-statistical value, while the lower-order terms provide a smooth interpolation to low pressures.

The characteristics of the cold curve $P_{\text{cold}}(V)$ and the Mie-Grüneisen equation of state (8.2) give a complete description of the caloric properties of a substance. The use of the quasiharmonic model of a solid in the Debye approximation also makes it possible to determine the temperature from (8.2) and from an expression which follows from (7.2):

$$E_{\text{latt}} = 3NkTD(x),$$

where $x = \hbar\omega_D/kT$ and

$$D(x) = \frac{3}{x^3}\int_0^x \frac{t^3\,dt}{e^t-1}.$$

This method has been used with shock-wave data on many substances to construct equations of state valid at megabar pressures.[146,168,169] The quasiharmonic model has also been modified[170] to incorporate the tensor nature of the equation of state.

With increasing temperature, the thermal vibrations of a lattice become anharmonic, and in the high-temperature limit the behavior of the lattice material is characterized by the properties of an ideal gas. These circumstances have been taken into account[171] by the addition to the free energy of a term

$$F_{\text{latt}} = \frac{3}{2}RT\ln(1+z), \tag{8.4}$$

where the quantity $z = lRT/c_{\text{cold}}^2$ is proportional to the ratio of the thermal and elastic parts of the pressure, and l is an empirical parameter found from experiments on the dynamic compression of porous samples. The equation of state constructed in this manner describes the transition from the condensed state ($z \approx 0$) to the ideal-gas state ($z \to \infty$).

A similar transition is described by the model of Ref. 172, where the substance is treated as an equilibrium mixture of harmonic oscillators and an ideal gas. The proportions in the mixture are determined by the conditions for thermodynamic equilibrium. Anharmonic effects are also taken into account by means of the free-volume theory[169] and by introducing a temperature-induced shift in the frequencies of the normal vibrational modes.[105]

The ideal-gas asymptotic behavior was achieved in Ref. 173 by describing the lattice heat capacity by the expression

$$C_V = \frac{3}{2}R\left[1 + \frac{1}{1+(0.1T/T_m)}\right],$$

which was found from data obtained by using simple models for a liquid: a system of soft spheres and a Coulomb plasma. Anharmonic effects in the cell model with the specific interaction potential

$$\varphi(r) = \frac{2ma^2\omega^2}{\pi^2}\operatorname{tg}^2\frac{\pi r}{2a},$$

which makes it possible to solve the Schrödinger equation exactly, have been incorporated in an equation of state.[174] This equation of state yields the correct gas asymptote in the limits $T \to \infty$ and $V \to \infty$, but it gives only a schematic description of dynamic experiments at high pressures.

With increasing temperature it becomes necessary to incorporate in the equations of state, along with lattice-anharmonicity effects, the contribution of thermally excited conduction electrons. This contribution is determined by the fine details of how the electron energy bands are filled, which are highly individual properties of each element (Section 5). The simplest way to incorporate the electron contribution in metals[15-18] is to

use the model of nearly free electrons, whose number is assumed to be constant and determined by the valence of the element. At pressures which are not too high the conduction electrons are degenerate, and their properties can be described by the model of an ideal Fermi gas,

$$E_e = \frac{\pi^2}{6}(kT)^2 \nu(\varepsilon_F), \quad P_e = \frac{\gamma_e}{V} E_e, \tag{8.5}$$

where $\nu(\varepsilon_F)$ is the density of electron states at the Fermi surface, and $\gamma_e = -\partial \ln \nu / \partial \ln V$. For a degenerate gas in the model of free electrons, we have $\gamma_e = 2/3$.

The values found for $\nu(\varepsilon_F)$ from low-temperature measurements of the heat capacity have usually turned out to be much lower than the predictions of the ideal-gas calculations. The discrepancy results from the approximate nature of the free-electron model, which becomes particularly arbitrary for transition metals with conduction electrons localized in a narrow d band. Direct quantum-mechanical calculations[84] show that compression causes a broadening and a transformation of the d band, while the state density at the Fermi surface changes dramatically. As a result, there are anomalies in the behavior of γ_e, which may even become negative.

The semiempirical models ignore the particular way in which the bands are filled, and they use the obviously simplified treatment of the electron terms according to which $\nu(\varepsilon_F)$ is taken from low-temperature experiments, while the Grüneisen electron coefficient is taken to be $\gamma_e = 1/2$ in accordance with the Thomas-Fermi theory.[168,169] This simplified approach is valid at substantial pressures, but at standard conditions it is an extremely crude approximation of the real situation. For metals at $T \sim 0$ the experimental values are $\gamma_e \approx 1-3$, and calculations[175] for aluminum and thorium show that the approximation $\gamma_e = 1/2$ is valid only at high temperatures ($T \sim 3 \cdot 10^4$ K). At temperatures $T \sim \varepsilon_F$ (which is of the order of 10^5 K for metals), the electron degeneracy is lifted, and (8.5) should be replaced by the exact relations for an ideal electron gas, (3.2). The semiempirical equations of state make it a far simpler matter to carry out specific calculations if the exact expressions for the electron terms are replaced by various approximations[157,171,176] which contain several adjustable parameters and which describe the correct asymptotic behavior at low and high temperatures.

In constructing equations of state of dielectrics, e.g., ionic crystals[177] and inert gases,[178] one must take into account the thermal excitation of electrons into the conduction band which occurs when a substance is heated. In this case the number of free electrons depends on the density and the temperature: $N_e \sim T^{3/2} \exp(-\Delta E/2kT)$, where $\Delta E(V)$ is the energy gap between the valence band and the conduction band. This gap is either specified by a model[177] or found by direct quantum-mechanical calculations[89] (Section 5). The term accounting for the contribution made by the free electrons in the expression for the free energy must be supplemented with an expression that takes into account the thermal excitation of the electrons.[177,178] Since compression narrows the energy gap, the additional term causes a negative increment in the pressure, with a magnitude which depends strongly on the rate at which the gap is narrowed[90] (Fig. 16).

The use of these expressions, or slight modifications of them, has resulted in the construction of equations of state for a large number of chemical elements and compounds.[168-174,176-178] The incorporation of anharmonic effects and electron effects has led to a satisfactory description of the thermodynamic characteristics of the condensed phase over a pressure range of tens of megabars. Other methods have also been proposed for constructing semiempirical equations of state. For example, the equation of state of water has been specified in the following form,[179] by analogy with (8.2):

$$E(P, V) = E_{\text{cold}}(P) + \frac{P}{\eta(P)}[V - V_{\text{cold}}(P)],$$

where the empirical dependence $\zeta(P) = P(\partial V/\partial E)_p$ is determined from experiments on the shock compression of ice and snow of various densities.

At high pressures, melting effects are estimated[180] to have only a slight influence on the kinematic characteristics in shock-wave experiments. Accordingly, the early semiempirical models ignored melting, with little effect on the calculations of the caloric characteristics observable experimentally. However, measurements of the temperature in shock-wave experiments[131,135] revealed a sensitivity of the temperature to melting (Fig. 27). Further study of metals with anomalous melting curves (Section 7) revealed that melting also affects the kinematic parameters of shock waves.[142] These circumstances and the need for an accurate calculation of the temperature in gasdynamic problems with heat conduction required an appropriate modification of the semiempirical models to incorporate melting correctly.

One way to incorporate melting in the semiempirical equations of state is to use the Lindemann criterion, with an entropy of melting, $\Delta S_m = 1.15R$, which is an average over all elements.[173,181,182] A more systematic way to take melting into account[157,177,180,183,184] is to add to the lattice term in the potential for the liquid phase some functions whose adjustable parameters accurately reproduce the experimental values of the changes in the entropy and density upon melting. This approach has

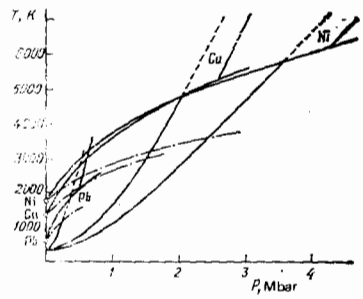

FIG. 32. Curves of the melting and temperature of the shock compression of lead, copper, and nickel.[180] Dashed curves—Superheated solid phase; dot-dashed curves—Lindemann melting law.

been used to calculate melting curves for ionic crystals[131,177] and metals[157,180,184] (Fig. 32). For hydrogen, the positions of the lines of the transition from the solid state to the liquid and from the molecular state to the metallic state have been determined[183] (Fig. 33). A method for calculating the melting curve and the lines of structural phase transitions from the slope of the experimental D-u dependence and static data is described in Ref. 142, where the phase boundaries are determined from the equilibrium conditions of the phases using the equations of state for each phase obtained from experimental data (Fig. 28).

A distinctive feature of the dynamic experiments from which the semiempirical models are constructed is that the experimental data determine the equation of state in the thermodynamically incomplete form $E = E(P, V)$, and in order to close the thermodynamics further information on the temperature, $T = T(P, V)$, is required.[14] This further information is extremely important for developing adequate semiempirical equations of state. For example, it was the measurement of the temperatures in dielectrics[131,177] which made it possible to determine the high-temperature part of the corresponding melting curves at record high pressures and to show that the quasiharmonic approximation is valid over a broad region of parameters all the way to the melting curve. It is an extremely difficult matter to measure the temperature during the shock loading of metals, which are optically opaque; only a few corresponding experiments have been carried out.[135] Consequently, indirect thermal information obtained by identifying the states in an isentropic unloading wave has become very important in constructing equations of state.[157,185]

A thermodynamically complete equation of state can be constructed from the data of dynamic experiments alone,[14,186] without appealing to any further model-based arguments regarding the properties or nature of the medium in question. This approach becomes possible if a sufficiently dense and uniform grid of experimental points is available over the parameter region of interest. An approximation of the experimental data determines the caloric equation of state,

$$E(P, V) = \sum_i \sum_j a_{ij} P^i V^j,$$

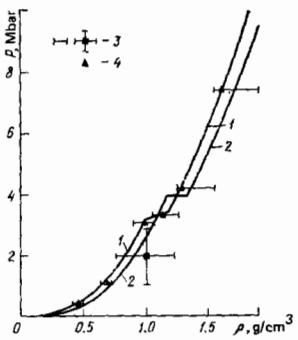

FIG. 33. Absolute-zero isotherms (1) and isentropes (2) of molecular and metallic hydrogen.[183] 3—Experimental data; 4—gasdynamic calculations.

and the temperature $T(P, V)$ is found by solving the linear, homogeneous differential equation

$$\left[P + \left(\frac{\partial E}{\partial V}\right)_P\right] \frac{\partial T}{\partial P} - \left(\frac{\partial E}{\partial P}\right)_V \frac{\partial T}{\partial V} = T \qquad (8.6)$$

by the method of characteristics. For condensed media[186], the results of static measurements at standard pressure have been used as initial data for Eq. (8.6); in the case of a cesium plasma,[53] data from low densities, at which the deviations from an ideal plasma are inconsequential, have been used for the same purpose. This approach has been used to construct equations of state for many substances[53,186]: cesium plasmas, metals of the basic and transition groups, ionic crystals, and silicon dioxide; Fig. 34 shows some representative results for tungsten.

Complete gasdynamic calculations on the events which occur during the high-temperature expansion of a substance have required the construction of semiempirical models which are valid over broad ranges of the parameters and which systematically incorporate evaporation effects. One method for describing the transition of a system from a condensed state to a gaseous state[181,182] is to combine the quasiharmonic model[173] with a modified van der Waals model of the liquid state.[116] This is purely a fitting procedure and does not provide a correct quantitative matching. At the same time, experimental data on the isentropic expansion of shock-compressed metals[157,185] provide the information required for developing semiempirical equations of state which give a quantitatively correct description of the liquid-vapor (or-plasma) transition.

Gasdynamic calculations across a broad range of physical conditions have required the development of equations of state which are valid over a broad range and which give a correct and thermodynamically complete description of the properties of the substance over an extensive part of the phase diagram, with a consistent account of melting, evaporation, dissociation, ionization, etc. An expansion of the range of applicability of the semiempirical equations of state to single out explicitly the physical asymptotic behavior has resulted in a significant complication of the terms of the thermodynamic potential in (8.1) and has increased the number of adjustable parameters, because of the need to describe the corresponding extreme situations. Various principles have been used to construct wide-range equations of state for many materials: metals,[157,176,184,187] water,[188-190] and sodium chloride.[188,191]

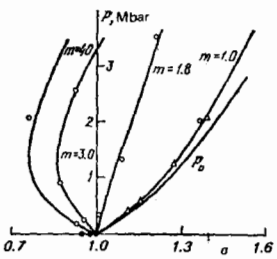

FIG. 34. Shock adiabatics (m) and cold curve (P_0) of tungsten.[186]

Figure 35 shows an example of a consistent description, from a common equation of state,[157] of some varied experimental data on lead: shock adiabatics, the sound velocity during shock loading and the temperature in an unloading wave. The agreement between the calculations of Ref. 157 and the experimental results is also illustrated by Fig. 36, which shows the theoretical and experimental data on the thermodynamic properties of aluminum in the critical region and in the liquid phase. From Figs. 35 and 36 we see an exact (within the experimental errors) agreement of the theoretical and experimental characteristics over broad ranges of the thermodynamic parameters—from standard conditions to pressures of hundreds of megabars. In addition to the satisfactory description of the varied experimental data, including data obtained under melting and evaporation conditions, the equations of state of aluminum,[184] copper, and lead[157] also take ionization into account and give the correct asymptotic behavior at high temperatures and large volumes. We wish to emphasize that the wide-range semiempirical equations of state presently available are the best method for a consistent and accurate description of the thermodynamics of substances over a broad part of the phase diagram. These equations of state generalize the results of experiments and model-based calculations.

We see from this review of model equations of state that the last two decades have seen much progress in methods for describing the thermodynamic properties of media in which there is a strong interparticle interaction. The progress in the development of new model equations of state has, in general, made it possible to describe the behavior of a substance in various states of aggregation—a description required for solving most problems in applied physics. Nevertheless, there are still many unmapped areas on the phase diagram, which at present do not seem accessible to study. We thus have a fertile soil for future theoretical and experimental research, which will call upon new ideas and new experimental methods. In this review we have attempted to draw a complete and up-to-date picture of the situation in this broad and rapidly developing field

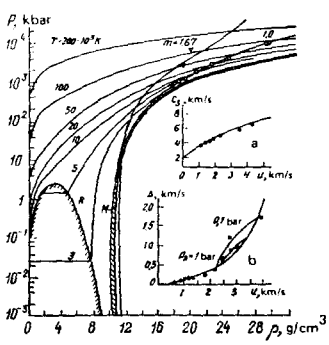

FIG. 35. Phase diagram of lead.[157] Points—Experimental; M—melting region; R—boiling curve; m—shock adiabatics (the dashed curves show the predictions of the Thomas-Fermi model); T—isotherms. a: Sound velocity on the shock adiabat. b: $\Delta = W - 2u$ in an isotropic unloading wave.

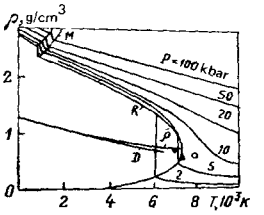

FIG. 36. Equation of state of aluminum in the near critical region.[157] M—melting region; R—boiling curve; D—rectilinear diameter; $\bar{\rho}$—half-sum of the densities of the liquid and gas phases; L—static measurements of the density of the liquid. Points: Critical points estimated from thermodynamic scaling principles.[156]

of modern physics.

We are deeply indebted to F. I. Dubovitskiĭ, A. M. Prokhorov, and A. E. Sheĭndlin for support, continuous interest, and stimulating discussions. We are also deeply indebted to L. P. Pitaevskiĭ, L. V. Al'tshuler, D. A. Kirzhnits, and E. G. Maksimov for useful comments offered in a reading of the manuscript.

[1)] The curves of the ground-state energies of the various phases as functions of r_s are very similar, and for this reason the positions of the transition points are highly sensitive to extremely small differences in the potentials.[36,37]

[2)] The density dependence of the pseudopotential has not been studied.

[3)] Optical measurements[54] also point to a substantial deformation of the energy spectrum of a dense plasma.

[4)] A qualitative improvement of the description at low pressures, reflecting the individuality of the various substances, has been achieved by using a model combining aspects of the quasiclassical and band theories.[73]

[5)] Arguments regarding the scaling of the dynamic adiabatic and dimensionless equations of state are given in Refs. 161–163.

[6)] The condition $\gamma/V = \text{const}$ causes γ to fall off very rapidly with the volume—in contradiction of other theories at a substantial degree of compression. Although the condition $\gamma/V^{1/2} = \text{const}$ is more suitable, it does not give the correct asymptotic result $\gamma = 2/3$ in the limit $V \to 0$. Finally, a direct experimental test of the applicability of the approximation $\gamma/V^q = \text{const}$ has been carried out for several metals at modest degrees of compression,[166] $V/V_0 \gtrsim 0.6$. The results for q cover the broad range from 0.6 (Fe) to 1.8 (In).

[1]E. A. Mason and T. H. Spurling (eds.), Virial Equation of State, Pergamon, New York, 1970 (Russ. Transl. Mir, Moscow, 1972).

[2]H. N. V. Temperley, J. S. Rowlinson and G. S. Rushbrooke (eds.), Physics of Simple Liquids, North Holland, Amsterdam, 1968 (Russ. Transl. Mir, Moscow, 1971).

[3]L. D. Landau and E. M. Lifshitz, Statisticheskaya fizika, Nauka, Moscow, 1976 (Statistical Physics, 3rd Ed., Pergamon Press, Oxford, 1980).

[4]G. É. Norman and A. N. Starostin, Teplofiz. Vys. Temp. 8, 413 (1970).

[5]W. Ebeling, W. Kraft, and D. Kramp, Theory of Bound States and the Polarization Equilibrium in Plasmas and Solids (Russ. Transl. Mir, Moscow, 1979).

[6]V. M. Ievlev (editor), Teplofizicheskie svoĭstva rabochikh sred gazofaznogo yadernogo reaktora (Thermophysical Properties of the Working Media of Gas-Phase Nuclear

Reactors), Atomizdat, Moscow, 1980.
[7]D. A. Kirzhnits, Yu. E. Lozovik, and G. V. Shpatakovskaya, Usp. Fiz. Nauk **117**, 3 (1975) [Sov. Phys. Usp. **18**, 649 (1975)].
[8]N. W. Ashcroft and N. D. Mermin, Solid State Physics, HR&W, 1976 (Russ. Transl. Mir, Moscow, 1979, Vols. 1, 2).
[9]N. W. Ashcroft and D. Stroud, Solid State Phys. **3**, 1 (1978).
[10]A. J. Barker and D. Henderson, Rev. Mod. Phys. **48**, 587 (1976).
[11]J. P. Hansen and I. R. McDonald, Theory of Simple Liquids, Academic Press, New York, 1976.
[12]N. K. Ailawadi, Phys. Rep. **57**, 243 (1980).
[13]S. M. Stishov, Usp. Fiz. Nauk **96**, 467 (1971); [*sic*]; **114**, 3 (1974) [Sov. Phys. Usp. **17**, 625 (1975)].
[14]Ya. B. Zel'dovich and Yu. P. Raĭzer, Fizika udarnykh voln i vysokotemperaturnykh gidrodinamicheskikh yavleniĭ, Nauka, Moscow, 1966 (Physics of Shock Waves and High-Temperature Hydrodynamic Phenomena, Academic Press, New York, 1966, 1967).
[15]L. V. Al'tshuler, Usp. Fiz. Nauk **85**, 197 (1965) [Sov. Phys. Usp. **8**, 52 (1966)].
[16]V. N. Zharkov and V. A. Kalinin, Uravneniya sostoyaniya tverdykh tel pri vysokikh davleniyakh i temperaturakh Nauka, Moscow, 1968 (Equations of State for Solids at High Pressures and Temperatures, Consultants Bureau, New York, 1971).
[17]S. G. Brush, Prog. High Temp. Phys. Chem. **1**, 3 (1967).
[18]P. Caldirola and H. Knoepfel (eds.), The Physics of High Energy Densities, Academic Press, New York, 1971 (Russ. Transl. Mir, Moscow, 1974).
[19]L. Davison and R. A. Graham, Phys. Rep. **55**, 265 (1979).
[20]Ya. B. Zel'dovich and I. D. Novikov, Relyativistskaya astrofizika (Relativistic Astrophysics), Nauka, Moscow, 1967.
[21]D. A. Kirzhnits, Usp. Fiz. Nauk **104**, 489 (1971) [Sov. Phys. Usp. **14**, 512 (1971)].
[22]N. H. March, S. Sampanthar and W. H. Young, The Many-Body Problem in Quantum Mechanics, Cambridge Univ. Press, 1967 (Russ. Transl. Mir, Moscow, 1969).
[23]G. Kalman (ed.) Strongly Coupled Plasmas, Plenum Press, New York, 1978; NATO Advanced Study Institutes Series, Vol. 36, Ser. B.
[24]M. Baus and J. -P. Hansen, Phys. Rep. **59**, 1 (1980).
[25]J. F. Springer, M. A. Pokrant, and F. A. Stevens, J. Chem. Phys. **58**, 4863 (1973).
[26]S. G. Brush, H. L. Sahlin, and E. Teller, J. Chem. Phys. **45**, 2102 (1966).
[27]J. P. Hansen, Phys. Rev. **A8**, 3096 (1973).
[28]W. L. Slattery, G. D. Doolen, and H. E. DeWitt, Phys. Rev. **21**, 2087 (1980); **26**, 2255 (1982).
[29]W. B. Hubbard and W. L. Slattery, Astrophys. J. **168**, 131 (1971).
[30]M. Ross and D. Seale, Phys. Rev. **A9**, 396 (1974); D. Stround and N. W. Ashcroft, Phys. Rev. **13**, 1660 (1976).
[31]V. K. Gryaznov and I. L. Iosilevskiĭ, Chislennye metody mekhaniki sploshnoĭ sredy (Numerical Methods in Continuum Mechanics), Vol. 4, No. 5, 1973, p. 166.
[32]J. L. Lebowitz and E. H. Lieb, Phys. Rev. Lett. **22**, 631 (1969).
[33]E. L. Pollock and J. P. Hansen, Phys. Rev. **A8**, 3110 (1973).
[34]A. A. Abrikosov, Zh. Eksp. Teor. Fiz. **39**, 1797 (1960) [Sov. Phys. JETP **12**, 1254 (1961)]; **41**, 569 (1961) [Sov. Phys. JETP **14**, 408 (1962)]; **45**, 2038 (1963) [Sov. Phys. JETP **18**, 1399 (1964)].
[35]E. P. Wigner, Trans. Faraday Soc. **34**, 678 (1938).
[36]W. J. Carr and A. A. Maradudin, Phys. Rev. **122**, 1437 (1961); **A133**, 371 (1964); G. Carmi, J. Math. Phys. **9**, 2120 (1968); K. Itsumi and S. Ichinaru, Phys. Rev. **B24**, 3220 (1981).
[37]D. Ceperley, Phys. Rev. **B18**, 3126 (1978); D. Ceperley and B. J. Alder, Phys. Rev. Lett. **45**, 566 (1980).
[38]O. V. Dolgov and E. G. Maksimov, Usp. Fiz. Nauk **135**, 441 (1981) [Rev. Mod. Phys. **53**, 81 (1981)].
[39]I. L. Iosilevskiĭ, in: Uravnenie sostoyaniya v ékstremal'nykh usloviyakh (G. V. Gadiyak, ed.) (Equation of State Under Extreme Conditions), ITPM SO Akad. Nauk SSSR, Novosibirsk, 1981, p. 20.
[40]M. A. Cook, R. T. Keyes, and L. L. Udy, J. Appl. Phys. **30**, 1881 (1959).
[41]V. E. Fortov, S. I. Musyankov, V. V. Yakushev, and A. N. Dremin, Teplofiz. Vys. Temp. **12**, 957 (1974).
[42]V. D. Gorobchenko and E. G. Maksimov, Usp. Fiz. Nauk **130**, 65 (1980) [Sov. Phys. Usp. **23**, 35 (1980)].
[43]Yu. G. Krasnikov and V. I. Kucherenko, Teplofiz. Vys. Temp. **16**, 43 (1978).
[44]F. J. Rogers, Phys. Rev. **A24**, 1531 (1981).
[45]H. C. Graboske, Jr., D. J. Harwood, and H. E. DeWitt, Phys. Rev. **3**, 1419 (1971).
[46]V. K. Gryaznov, I. L. Iosilevskiĭ, and V. E. Fortov, Zh. Prikl. Mekh. Tekh. Fiz. No. 3, 70 (1973).
[47]V. M. Zamalin, G. É. Norman, and V. S. Filinov, Metod Monte-Karlo v statisticheskoĭ termodinamike (The Monte Carlo Method in Statistical Thermodynamics), Nauka, Moscow, 1977.
[48]A. I. Larkin, Zh. Eksp. Teor. Fiz. **38**, 1896 (1960) [Sov. Phys. JETP **11**, 1363 (1961)].
[49]A. G. Khrapak and I. T. Yakubov, Zh. Eksp. Teor. Fiz. **69**, 2042 (1975) [Sov. Phys. JETP **42**, 1036 (1975)].
[50]A. Yu. Savukinas and A. Z. Chizhyunas, Litov. Fiz. Sb. **14**, 73 (1974).
[51]H. C. Graboske, Jr., D. J. Harwood, and F. J. Rogers, Phys. Rev. **186**, 210 (1969).
[52]V. K. Gryaznov, M. V. Zhernokletov, V. N. Zubarev, I. L. Iosilevskiĭ, and V. E. Fortov, Zh. Eksp. Teor. Fiz. **78**, 573 (1980) [Sov. Phys. JETP **51**, 288 (1980)]; in: Ref. 6, p. 41.
[53]A. V. Bushman, B. N. Lomakin, V. A. Sechenov, V. E. Fortov, I. I. Sharipdzhanov, and O. E. Shchekotov, Zh. Eksp. Teor. Fiz. **69**, 1624 (1975) [Sov. Phys. JETP **42**, 828 (1975)].
[54]V. E. Bespalov, V. K. Gryaznov, and V. E. Fortov, Zh. Eksp. Teor. Fiz. **76**, 140 (1979) [Sov. Phys. JETP **49**, 71 (1979)].
[55]B. K. Godwal, S. K. Sikka, and R. Chidambaram, Phys. Rev. Lett. **47**, 1144 (1981); B. K. Godwal and S. K. Sikka, J. Phys. F **12**, 655 (1982).
[56]I. L. Iosilevskiĭ, Teplofiz. Vys. Temp. **18**, 447 (1980); in: Ref. 6, p. 176.
[57]V. P. Kopyshev, Dokl. Akad. Nauk SSSR **161**, 1067 (1965) [Sov. Phys. Dokl. **10**, 338 (1965)].
[58]R. Latter, Phys. Rev. **99**, 1854 (1955).
[59]N. N. Kalitkin and L. V. Kuz'mina, Preprint No. 35, IPM AN SSSR, Moscow, 1975; N. N. Kalitkin, Author's Abstract, Doctorate Dissertation, IPM AN SSSR, Moscow, 1975.
[60]D. A. Kirzhnits and G. V. Shpatakovskaya, Zh. Eksp. Teor. Fiz. **62**, 2082 (1972) [Sov. Phys. JETP **35**, 1088 (1972)].
[61]D. A. Kirzhnits, Zh. Eksp. Teor. Fiz. **32**, 115 (1957) [Sov. Phys. JETP **5**, 64 (1957)].
[62]R. M. More, Phys. Rev. **A19**, 1234 (1979).
[63]F. Perrot, Physica (Utrecht) **A98**, 555 (1979); Phys. Rev. **A20**, 586 (1979).
[64]I. L. Iosilevskiĭ and V. K. Gryaznov, Teplofiz. Vys. Temp. **19**, 1121 (1981).
[65]A. F. Nikiforovov, V. G. Novikov, Yu. N. Orlov, and V. B. Uvarov, Preprint No. 172, IPM AN SSSR, Moscow, 1979.
[66]R. M. More and S. Skupsky, Phys. Rev. **A14**, 474 (1976).
[67]R. F. Trunin, M. A. Podurets, G. V. Simakov, L. V. Popov, and B. N. Moiseev, Zh. Eksp. Teor. Fiz. **62**, 1043 (1972) [Sov. Phys. JETP **35**, 550 (1972)].
[68]C. E. Ragan, M. G. Silbert, and B. C. Diven, J. Appl. Phys. **48**, 2860 (1977); C. E. Ragan, Phys. Rev. **A21**, 458 (1980); **25**, 3360 (1982).
[69]V. N. Zubarev, M. A. Podurets, L. V. Popov, G. V. Simakov,

and R. F. Trunin, in: Detonatsiya (Detonation), OIKhF AN SSSR, Chernogolovka, Mosk. obl., 1968, p. 61.
[70]L. P. Volkov, N. P. Voloshin, A. S. Vladimirov, V. N. Nogin, and V. A. Simonenko, Pis'ma Zh. Eksp. Teor. Fiz. **31**, 623 (1980) [JETP Lett. **31**, 588 (1980)].
[71]E. N. Avrorin, B. K. Vodolaga, L. P. Volkov, A. S. Vladimirov, V. A. Simonenko, and B. T. Chernovolok, Pis'ma Zh. Eksp. Teor. Fiz. **31**, 727 (1980) [JETP Lett. **31**, 685 (1980)].
[72]L. V. Al'tshuler, N. N. Kalitkin, L. V. Kuz'mina, and B. S. Chekin, Zh. Eksp. Teor. Fiz. **72**, 317 (1977) [Sov. Phys. JETP **45**, 167 (1977)].
[73]D. A. Liberman, Phys. Rev. **B20**, 4981 (1979).
[74]N. N. Kalitkin and I. A. Govorukhina, Fiz. Tverd. Tela (Leningrad) **7**, 355 (1965) [Sov. Phys. Solid State **7**, 287 (1965)].
[75]C. M. Lee and E. I. Thorsos, Phys. Rev. **A17**, 2073 (1978).
[76]G. V. Sin'ko, Chislennye Metody Mekhaniki Sploshnoĭ Sredy **10**, No. 1, 124 (1979); **12**, No. 1, 121 (1981).
[77]A. K. McMahan and M. Ross, in: High Pressure Science and Technology (ed. K. D. Timmerhaus and M. S. Barber), Vol. 2, Plenum Press, New York, 1979, p. 920.
[78]E. H. Lieb and B. Simon, Phys. Rev. Lett. **31**, 681 (1973).
[79]R. J. Trainor, J. W. Shaner, J. M. Auerbach, and N. C. Holmes, Phys. Rev. Lett. **42**, 1154 (1979); L. R. Veeser, J. C. Solem, and A. J. Lieber, Appl. Phys. Lett. **35**, 761 (1979).
[80]J. M. Ziman, The Calculation of Bloch Functions, Solid State Phys. 26, 1 (1971) (Russ. Transl. Mir, Moscow, 1973).
[81]V. Heine, M. L. Cohen, and D. Weaire, Theory of Pseudopotentials. in: Solid State Physics, Vol. 24 (ed. H. Ehrenreich, F. Seitz, and D. Turnbull), Academic Press, New York, 1970 (Russ. Transl. Mir, Moscow, 1973).
[82]M. Born and K. Huang, Dynamical Theory of Crystal Lattices, Oxford Univ. Press, 1954 (Russ. Transl. Mir, Moscow, 1958).
[83]E. G. Brovman and Yu. Kagan, Usp. Fiz. Nauk **112**, 369 (1974) [Sov. Phys. Usp. **17**, 125 (1974)].
[84]A. I. Voropinov, G. M. Gandel'man, and V. G. Podval'nyĭ, Usp. Fiz. Nauk **100**, 193 (1970) [Sov. Phys. Usp. **13**, 56 (1970)]; L. V. Al'tshuler, A. I. Voropinov, G. M. Gandel'man, N. A. Dmitriev, and V. G. Podval'nyĭ, Fiz. Met. Metalloved. **51**, 76 (1981).
[85]L. V. Al'tshuler and A. A. Bakanova, Usp. Fiz. Nauk 96, 193 (1968) [Sov. Phys. Usp. **11**, 678 (1970)].
[86]J. C. Slater, in: Advances in Quantum Chemistry, Vol. 6, Academic Press, 1972, p. 1.
[87]B. F. Rozsnayi, Phys. Rev. **A5**, 1137 (1972).
[88]N. A. Dmitriev and V. G. Podval'nyĭ, Fiz. Met. Metalloved. **52**, 28 (1981).
[89]A. K. McMahan, B. L. Hord, and M. Ross, Phys. Rev. **B15**, 718, 726 (1977); A. K. McMahan, Phys. Rev. **17**, 1521 (1978).
[90]M. Ross and A. K. McMahan, Phys. Rev. **21**, 1658 (1980).
[91]O. K. Anderson, Phys. Rev. **12**, 3060 (1975).
[92]F. Hohenberg and W. Kohn, Phys. Rev. **B136**, 864 (1964); W. Kohn and L. J. Sham, Phys. Rev. **A140**, A1133 (1965).
[93]A. K. McMahan, H. L. Skriver, and B. Johansson, Phys. Rev. **B23**, 5016 (1981).
[94]H. L. Skriver and J. -P. Jan, Phys. Rev. **21**, 1489 (1980).
[95]J. -P. Jan and H. L. Skriver, J. Phys. F **11**, 805 (1981).
[96]F. Perrot, Phys. Status Solidi **b101**, 741 (1980).
[97]D. Glötzel and A. K. McMahan, Phys. Rev. **B20**, 3210 (1979).
[98]U. K. Poulsen, J. Kollar, and O. K. Andersen, J. Phys. F **6**, L241 (1976).
[99]D. Glötzel, J. Phys. F **8**, L163 (1978).
[100]H. L. Skriver, O. K. Andersen, and B. Johansson, Phys. Rev. Lett. **41**, 42 (1978); **44**, 1230 (1980).
[101]V. G. Vaks, S. P. Kravchuk, and A. V. Trefilov, Fiz. Tverd. Tela (Leningrad) **19**, 1271, 3396 (1977) [Sov. Phys. Solid State **19**, 740, 1983 (1977)]; **21**, 3370 (1979) [Sov. Phys. Solid State **21**, 1945 (1979)].
[102]T. Soma and H. Satoh, Phys. Status Solidi **b107**, K25 (1981); J. Phys. F **10**, 1081, 1401 (1980).
[103]S. K. Sarkar and D. Sen, J. Phys. F **11**, 377 (1981); Phys. Rev. **B22**, 1856 (1980).
[104]Yu. Kagan, V. V. Pushkarev, and A. Kholas, Zh. Eksp. Teor. Fiz. **73**, 967 (1977) [Sov. Phys. JETP **46**, 511 (1977)].
[105]D. J. Pastine and M. J. Carrol, in: Accurate Characterization of the High Pressure Environment (ed. E. C. Lloyd), U. S. Government Printing Office, Washington, 1971, p. 91.
[106]H. H. Demarest, Jr., J. Phys. Chem. Solids **35**, 1393 (1974).
[107]V. A. Zhdanov and V. V. Polyakov, Zh. Prikl. Mekh. Tekh. Fiz. No. 5, 123 (1976); No. 4, 102 (1979).
[108]H. Eyring and M. S. Jhon, Significant Liquid Structures Ch. 2, 3, Wiley, New York, 1969.
[109]B. Steffen and R. Hosemann, Phys. Rev. **B13**, 3232 (1976).
[110]E. R. Cowley and J. A. Barker, J. Chem. Phys. **73**, 3452 (1980).
[111]G. A. Mansoori and F. B. Canfield, J. Chem. Phys. **51**, 4958 (1969).
[112]H. C. Andersen, D. Chandler, and J. D. Weeks, Adv. Chem. Phys. **34**, 109 (1976).
[113]F. H. Ree, in: Physical Chemistry. An Advanced Treatise: Liquid State (ed. H. Eyring, D. Henderson, and W. Yost), Vol. 8A, Ch. 3, Academic Press, New York, 1971.
[114]W. G. Hoover and M. Ross, Contemp. Phys. **12**, 339 (1971); W. G. Hoover, G. Stell, E. Goldmark, and G. D. Degani, J. Chem. Phys. **63**, 5434 (1975).
[115]D. A. Young and B. J. Alder, J. Chem. Phys. **70**, 473 (1979); **73**, 2430 (1980).
[116]D. A. Young and B. J. Alder, Phys. Rev. **A3**, 364 (1971).
[117]G. R. Gathers, J. W. Shaner, and D. A. Young, Phys. Rev. Lett. **33**, 70 (1974); D. Young, Report UCRL-52352, Univ. Calif., Livermore, 1977.
[118]G. R. Gathers, J. W. Shaner, R. S. Hixson, and D. A. Young, High Temp. High Press. **11**, 653 (1979).
[119]M. Ross, Phys. Rev. **B21**, 3140 (1980).
[120]M. Ross, J. Chem. Phys. **71**, 1576 (1979).
[121]M. Ross, J. Chem. Phys. **73**, 4445 (1980).
[122]D. Young and M. Ross, J. Chem. Phys. **74**, 6950 (1981).
[123]D. Young, A. K. McMahan, and M. Ross, Phys. Rev. **B24**, 5119 (1981).
[124]M. Ross, H. E. DeWitt, and W. B. Hubbard, Phys. Rev. **B24**, 1016 (1981).
[125]K. K. Mon, R. Gann, and D. Stroud, Phys. Rev. **24**, 2145 (1981).
[126]G. I. Kerley, J. Chem. Phys. **73**, 469, 478, 487 (1980).
[127]G. I. Kerley and J. Abdallah, Jr., J. Chem. Phys. **73**, 5337 (1980).
[128]R. D. Dick and G. I. Kerley, J. Chem. Phys. 73, 5264 (1980).
[129]S. M. Stishov, I. N. Makarenko, and A. M. Nikolaenko, Pis'ma Zh. Eksp. Teor. Fiz. **32**, 40 (1980) [JETP Lett. **32**, 37 (1980)].
[130]L. D. Landau, Zh. Eksp. Teor. Fiz. **7**, 627 (1937).
[131]S. B. Kormer, Usp. Fiz. Nauk **94**, 641 (1968) [Sov. Phys. Usp. **11**, 229 (1968)].
[132]I. N. Makarenko, A. M. Nikolaenko, and S. M. Stishov, Zh. Eksp. Teor. Fiz. **74**, 2175 (1978) [Sov. Phys. JETP **47**, 1132 (1978)].
[133]P. W. Mirwald, Cited in Ref. 77, Vol. 1, p. 361.
[134]V. Ya. Vashchenko and V. N. Zubarev, Fiz. Tverd. Tela (Leningrad) **5**, 886 (1963) [Sov. Phys. Solid State 5, 653 (1963)].
[135]R. A. Urtiew and R. Grover, J. Appl. Phys. **48**, 1122 (1977).
[136]M. Ross, Phys. Rev. **184**, 233 (1969).
[137]V. V. Palciauskas, J. Phys. Chem. Solids **37**, 571 (1976); **40**, 787 (1979).
[138]Yu. Ya. Boguslavskiĭ, F. F. Voronov, M. A. Il'ina, and O. V. Stal'gorova, Zh. Eksp. Teor. Fiz. **77**, 946 (1979) [Sov. Phys. JETP **50**, 476 (1979)].
[139]E. Rapoport, J. Chem. Phys. **46**, 2891 (1967); **48**, 1433

(1968).
[140]L. V. Al'tshuler, A. A. Bakanova, and I. P. Dudoladov, Zh. Eksp. Teor. Fiz. **53**, 1967 (1967) [Sov. Phys. JETP **26**, 1115 (1968)].
[141]W. H. Gust and E. B. Royce, Phys. Rev. **B8**, 3595 (1973).
[142]W. J. Carter, J. N. Fritz, S. P. Marsh, and R. G. McQueen, J. Phys. Chem. Solids **36**, 741 (1975).
[143]R. Grover and B. J. Alder, J. Phys. Chem. Solids **35**, 753 (1974).
[144]H. K. Mao, R. M. Hazen, P. M. Bell, and J. Wittig, J. Appl. Phys. **52**, 4572 (1981).
[145]E. Yu. Tonkov, Fazovye diagrammy élementov pri vysokom davlenii (High-Pressure Phase Diagrams of the Elements), Nauka, Moscow, 1979.
[146]R. G. McQueen, S. P. Marsh, J. W. Taylor, J. N. Fritz, and W. J. Carter, in: High Velocity Impact Phenomena (ed. R. Kinslow), Academic Press, New York, 1970, p. 293.
[147]L. V. Al'tshuler, A. A. Bakanova, I. P. Dudoladov, E. A. Dynin, R. F. Trunin, and B. S. Chekin, Zh. Prikl. Mekh. Tekh. Fiz. No. 2, 3 (1981).
[148]D. G. Pettifor, J. Phys. C **3**, 367 (1970); J. A. Moriarty and A. K. McMahan, Phys. Rev. Lett. **48**, 809 (1982).
[149]J. C. Duthie and D. G. Pettifor, Phys. Rev. Lett. **38**, 564 (1977).
[150]Y. K. Vohra, H. Olejnik, W. Grosshans, and W. B. Holzapfel, Phys. Rev. Lett. **47**, 1065 (1981).
[151]B. Johansson, J. Phys. Chem. Solids **39**, 467 (1978).
[152]R. A. Stager and H. G. Drickamer, Phys. Rev. **133**, 830 (1964).
[153]I. M. Lifshitz, Zh. Eksp. Teor. Fiz. **38**, 1569 (1960) [Sov. Phys. JETP **11**, 1130 (1961)].
[154]R. B. Roff, R. G. Haire, D. Schiferl, L. A. Schwalbe, E. A. Kmetko, and J. L. Smith, Science **207**, 1353 (1981).
[155]V. E. Fortov, A. N. Dremin, and A. A. Leont'ev, Teplofiz. Vys. Temp. **13**, 1072 (1975).
[156]R. W. Ohse and H. Tippelskirch, High Temp. High Press. **9**, 376 (1977).
[157]L. V. Al'tshuler, A. V. Bushman, M. V. Zhernokletov, V. N. Zubarev, A. A. Leont'ev, and V. E. Fortov, Zh. Eksp. Teor. Fiz. **78**, 741 (1980) [Sov. Phys. JETP **51**, 373 (1980)].
[158]U. Seydel and W. Fucke, J. Phys. F **8**, L157 (1978); High Temp. High Press. **12**, 419 (1980).
[159]M. Gitterman and V. Steinberg, Phys. Rev. Lett. **35**, 1588 (1975).
[160]L. D. Landau and Ya. B. Zel'dovich, Zh. Eksp. Teor. Fiz. **14**, 32 (1944).
[161]F. E. Prieto, J. Phys. Chem. Solids **35**, 279 (1974); **36**, 871 (1975); F. E. Prieto and C. Renero, J. Phys. Chem. Solids **37**, 151 (1976); **43**, 147 (1982).
[162]B. S. Chekin, Zh. Prikl. Mekh. Tekh. Fiz. No. 2, 89 (1978).
[163]V. F. Anisichkin, Zh. Prikl. Mekh. Tekh. Fiz. No. 3, 117 (1978).
[164]J. P. Romain, A. Migault, and J. Jacquesson, J. Phys. Chem. Solids **37**, 1159 (1976); **41**, 323 (1980); Cited in Ref. 77, Vol. 1, p. 99.
[165]T. Neal, Phys. Rev. **B14**, 5172 (1976).
[166]R. Boehler and J. Ramakrishnan, J. Geophys. Res. **B85**, 4996 (1980).
[167]M. Delannoy and G. Perrin, J. Phys. Chem. Solids **41**, 11 (1980).
[168]S. B. Kormer and V. D. Urlin, Dokl. Akad. Nauk SSSR **131**, 542 (1960) [Sov. Phys. Dokl. **5**, 317 (1960)]; S. B. Kormer, V. D. Urlin, and L. T. Popova, Fiz. Tverd. Tela (Leningrad) **3**, 2131 (1961) [Sov. Phys. Solid State **3**, 1547 (1962)].
[169]L. V. Al'tshuler, S. B. Kormer, A. A. Bakanova, and R. F. Trunin, Zh. Eksp. Teor. Fiz. **38**, 790 (1960) [Sov. Phys. JETP **11**, 573 (1960)]; **42**, 91 (1962) [*sic*].
[170]V. A. Zhdanov and A. V. Zhukov, Zh. Prikl. Mekh. Tekh. Fiz. No. 5, 139 (1978).
[171]S. B. Kormer, A. I. Funtikov, V. D. Urlin, and A. N. Kolesniko, Zh. Eksp. Teor. Fiz. **42**, 686 (1962) [Sov. Phys. JETP **15**, 477 (1962)].
[172]R. Gasnier, in: Symposium HDP, Dunod, Paris, 1968.
[173]R. Grover, J. Chem. Phys. **55**, 3435 (1971); Cited in Ref. 77, Vol. 1, p. 33.
[174]R. J. Naumann, J. Appl. Phys. **42**, 4945 (1971).
[175]B. K. Godwal, S. K. Sikka, and R. Chidambaram, Phys. Rev. **B20**, 2362 (1979); B. K. Godwal and S. K. Sikka, J. Phys. F **10**, 377 (1980).
[176]A. T. Sapozhnikov and A. V. Pershina, Voprosy at. nauki i tekhniki. Ser. Metodika i programmy resheniya zadach matematicheskoĭ fiziki (Questions of Atomic Sciences and Engineering. Series on Methods and Programs for Solving Problems of Mathematical Physics), Vol. 3, 1979, p. 37.
[177]S. B. Kormer, M. V. Sinitsyn, G. A. Kirillov, and V. D. Urlin, Zh. Eksp. Teor. Fiz. 48, 1033 (1965) [Sov. Phys. JETP **21**, 689 (1965)].
[178]M. Ross, Phys. Rev. **171**, 777 (1968).
[179]A. A. Bakanova, V. N. Zubarev, Yu. N. Sutulov, and R. F. Trunin, Zh. Eksp. Teor. Fiz. 68, 1099 (1975) [Sov. Phys. JETP **41**, 544 (1975)].
[180]V. D. Urlin and A. A. Ivanov, Dokl. Akad. Nauk SSSR 149, 1303 (1963) [Sov. Phys. Dokl. **8**, 380 (1963)]; V. D. Urlin, Zh. Eksp. Teor. Fiz. 49, 485 (1965) [Sov. Phys. JETP 22, 341 (1966)].
[181]D. A. Young, in: Report UCRL-51575, Univ. Calif., Livermore, 1974.
[182]C. Boissiere and G. Fiorese, Rev. Phys. Appl. **12**, 857 (1977).
[183]F. V. Grigor'ev, S. B. Kormer, O. L. Mikhaĭlova, A. P. Tolochko, and V. D. Urlin, Zh. Eksp. Teor. Fiz. 75, 1683 (1978) [Sov. Phys. JETP **48**, 847 (1978)].
[184]A. V. Bushman, A. L. Ni, and V. E. Fortov, Cited in Ref. 39, p. 3.
[185]L. V. Al'tshuler, A. A. Bakanova, A. V. Bushman, I. P. Dudoladov, and V. N. Zubarev, Zh. Eksp. Teor. Fiz. **73**, 1866 (1977) [Sov. Phys. JETP **46**, 980 (1977)].
[186]V. E. Fortov, Zh. Prikl. Mekh. Tekh. Fiz. No. 6, 156 (1972); Fiz. Goreniya Vzryva **8**, 428 (1972).
[187]A. V. Bushman, V. E. Fortov, and I. I. Sharipdzhanov, Teplofiz. Vys. Temp. **15**, 1095 (1977).
[188]N. N. Kalitkin, L. V. Kuz'mina, and I. I. Sharipdzhanov, Preprint No. 43, IPM AN SSSR, Moscow, 1976.
[189]S. V. Bobrovskiĭ, V. M. Gogolev, M. G. Menzhulin, and R. P. Shilovs, Zh. Prikl. Mekh. Tekh. Fiz. No. 5, 130 (1978).
[190]G. V. Kovalenko and A. T. Sapozhnikov, Voprosy at. nauki i tekhniki. Ser. Metodika i programmy resheniya zadach matematicheskoĭ fiziki (Questions of Atomic Science and Engineering. Series on Methods and Programs for Solving Problems of Mathematical Physics), Vol. 3, 1979, p. 93.
[191]S. V. Bobrovskiĭ, V. M. Gogolev, V. V. Zamyshlyaev, and V. P. Lozhkina, Zh. Prikl. Mekh. Tekh. Fiz. No. 6, 112 (1979).
[192]K. Syassen, Phys. Rev. **A25**, 6548 (1982); K. Asaumi, T. Mori, and Y. Kondo, Phys. Rev. Lett. **49**, 837 (1982).
[193]Y. K. Vohra, W. Grosshans, and W. B. Holzapfel, Phys. Rev. **B25**, 6019 (1982).
[194]Y. K. Bohra and W. B. Holzapfel, Phys. Lett. A89, 149 (1982).
[195]W. Hefner and F. Hensel, Phys. Rev. Lett. **48**, 1026 (1982).
[196]K. Syassen, G. Wortmann, J. Feldhaus, K. H. Frank, and G. Kaindl, Phys. Rev. **B26**, 4745 (1982).
[197]D. I. Khomskiĭ, Usp. Fiz. Nauk **129**, 443 (1979) [Sov. Phys. Usp. **22**, 879 (1979)].
[198]W. A. Grosshans, Y. K. Bohra, and W. B. Holzapfel, Phys. Rev. Lett. **49**, 1572 (1982).
[199]D. Glötzel, in: Physics of Solids Under High Pressure (ed. J. Schillinger and R. Shelton), North Holland, Amsterdam, 1981, p. 263.

Translated by Dave Parsons